Fall 1-27-2008

The use of instrumented measures to describe lower extremity joint mechanics

Steven Thomas Kaufman
New Jersey Institute of Technology

ABSTRACT

THE USE OF INSTRUMENTED MEASURES TO DESCRIBE LOWER EXTREMITY JOINT MECHANICS

by

Steven Thomas Kaufman

Currently, various biomechanical assessments are used in clinical settings that offer diagnostic information about the studied joint. These assessments, however, are based on the judgment and experience of the therapist conducting the test and have a high degree of inter and intra rater variability, decreasing the strength of the observation. A set of instrumented measures consisting of a force/torque sensor and an angle sensor was created to quantitatively assess the mechanics of the lower extremity joints as a possible solution to the low repeatability of commonly used clinical tests.

It was shown through the use of instrumentation that the torques about the lower leg joint during passive movement could be accurately measured with a high degree of repeatability in a variety of conditions, and that the torque measured by the force sensor matches those calculated by the angle sensor using the inverse kinematic equation for a damped pendulum. By knowing the kinematic torques occurring during the movement, any extra torque generated by pathological involuntary muscle contraction can be accurately quantified for a better description of the biomechanics of the joint under passive movement conditions.

THE USE OF INSTRUMENTED MEASURES TO DESCRIBE LOWER EXTREMITY JOINT MECHANICS

by
Steven Thomas Kaufman

A Thesis
Submitted to the Faculty of
New Jersey Institute of Technology
in Partial Fulfillment of the Requirements for the Degree of
Master of Science in Biomedical Engineering

Department of Biomedical Engineering

January 2008

APPROVAL PAGE

THE USE OF INSTRUMENTED MEASURES TO DESCRIBE LOWER EXTREMITY JOINT MECHANICS

Steven Thomas Kaufman

Dr. Richard Foulds, Thesis Advisor — Date
Associate Professor of Biomedical Engineering, NJIT

Dr. Sergei Adamovich, Committee Member — Date
Assistant Professor of Biomedical Engineering, NJIT

Dr. Bruno Mantilla, Committee Member — Date
Special Lecturer of Biomedical Engineering, NJIT

BIOGRAPHICAL SKETCH

Author: Steven Thomas Kaufman

Degree: Master of Science

Date: January 2008

Undergraduate and Graduate Education:

- Master of Science in Biomedical Engineering,
  New Jersey Institute of Technology, Newark, NJ, 2008

- Bachelor of Science in Biomedical Engineering,
  Syracuse University, Syracuse, NY, 2006

Major: Biomedical Engineering

To my beloved family for supporting me and providing guidance throughout the years as I strive to further my education.

ACKNOWLEDGMENT

I would like to express my deepest appreciation to Dr. Richard Foulds, not only for his willingness to take me on as a thesis student, but also for guiding me through my graduate education to where I needed to be to obtain my degree. Special thanks are given to Dr. Sergei Adamovich, and Dr. Bruno Mantilla for actively participating in my committee.

Many of my fellow graduate students in the Neuromuscular Engineering Lab also deserve recognition for their assistance throughout the past year and a half. I would also like to specifically thank Katherine Swift and Amanda Irving, who assisted in developing the MATLAB code for this thesis and essentially made this project possible.

TABLE OF CONTENTS

TABLE OF CONTENTS
(Continued)

LIST OF TABLES

LIST OF FIGURES

LIST OF SYMBOLS

EMG	Electromyography
FOB	Flock of Birds Sensor
FT	Force/Torque Sensor
AS	Ashworth Scale
MAS	Modified Ashworth Scale
GABA	Gamma-Aminobutyric acid
CP	Cerebral Palsy
ATP	Adenosine Triphosphate
N	Newton
M	Meter
ROM	Range of Motion
$I = m*p^2 + m*x^2$	Mass Moment of Inertia
$M_{applied}=I*\alpha+\beta*\omega+k(\Delta\theta)+m*g*l*\sin(\theta)$	Kinematic Equation

CHAPTER 1

INTRODUCTION

1.1 Objective

The objective of this thesis is to develop a new biomechanical measure of joint resistance that allows for quantifiable and repeatable results as a supplement to the Ashworth (AS), Modified Ashworth (MAS), and Tardieu scales with the testing procedures mimicking that of these commonly used tests for spasticity.

For this new biomechanical measure of joint resistance/torque, two pieces of measurement instrumentation will be used to obtain joint torque measurements through a force sensor, and joint angle, angular velocity, and acceleration measurements through an angle/position sensor. All of the results will undergo filtering and processing to better demonstrate how instrumented measures will allow for a more precise assessment of the joint mechanics associated with spasticity than the AS, MAS and Tardieu scales.

For the biomechanical assessment of the joint, the following points of data will be described and derived: (1) Measured joint torque of the limb vs. time, (2) calculated theoretical joint torque vs. time, (3) angle vs. time, and (4) angular velocity vs. time.

1.2 Background Information

This project will be examining the passive biomechanics of various joints in the human body. A joint is a physiological intersection of two or more bone segments and depending on the location and type of joint, varying degrees of freedom of motion can result from this intersection. At the location where the bones meet there are tendons and

ligaments spanning the connection, and the bony ends are covered with a very resilient and low friction covering (cartilage) comprised of collagen that allows for smooth rotation and translation of one bony end relative to the other (Widmaier 2004). The joints being examined in this study are those that rotate in one plane about a fixed axis (elbow and knee). In this case, the joint either moves in flexion or extension, and there are two groups of muscles, flexors and extensors that will lengthen and shorten depending on the direction of movement. The muscle groups are located on either side of the proximal limb segment (femur and humerus), with the upper limb muscles being the biceps (flexors) and the triceps (extensors) and the lower limb muscles being the hamstrings (flexors) and the quadriceps (extensors).

The muscles are a network of contractile units encased in connective collagen tissue that when stimulated, shorten by way of cross linking between the two main proteins that comprise the muscle unit or sarcomere. The proteins, actin and myosin, link and release by way of cross bridges in the presence of ATP, and the cross bridges undergo a ratchet and pull mechanism when there is also an influx of calcium ions from the sarcoplasmic reticulum, which is released when there is sufficient acetylcholine (neurotransmitter) present at the neuromuscular junction (Widmaier 2004). The ends of the muscle contain less contractile units and a higher percentage of connective tissue, until a complete transition to connective tissue has occurred at the extreme ends of the muscle, called the tendon. The tendon is responsible for attaching the muscle to the bone. One tendon is anchored to the same bone (humerus or femur) in which the muscle is located, and the tendon at the other end of the muscle spans the joint and attaches to the distal limb segment bone (radius/ulna or tibia/fibula). The tendon attaches in a location

on the distal segment some distance away from the joint at an angle which varies from person to person. The distance between the joint and the tendon attachment is essentially a moment arm, capable of generating torque under certain conditions (Winter 2005). When the muscle contracts and shortens, it creates tension in the tendon, and pulls on the distal segment in a manner so that a force (torque) is generated to rotate the segments relative to each other, and also a normal force is generated by the contraction, pulling the distal segment in a direction towards the proximal segment which stabilizes the joint. Since there are two muscle sets on either side of the proximal segment, they rotate the joint in opposite directions and are called an agonist/antagonist pair.

The signals generated by the brain travel down the cortiospinal tract by way of the upper motor neurons to the brainstem and spinal cord, and the lower motor neuron carries the signal from the brainstem and spinal cord to the neuromuscular junction where it terminates. Muscles are innervated by both sensory and motor neurons that send both movement commands and proprioceptive feedback to and from the brain at the same time. The muscle spindles are responsible for sensing information from the muscle and relaying it back to the central nervous system, and these structures are located in the fleshy, extrafusal muscle fibers (Botterman et al 1978). They number from three to ten intrafusal muscle fibers encapsulated in connective tissues and are aligned parallel to the extrafusal muscle fibers. These structures are activated by stretch sensitive ion channels. As with skeletal muscle, tendons also contain organs that send feedback signals to the spinal cord that monitor the tension measured in the tendon. These signals may be acted upon by reflexes that are in place to stop a limb from moving at a speed or to a position which the body deems dangerous or when the tension in the tendon becomes dangerous

and will subsequently activate the antagonist muscle responsible for slowing and stopping the limb's movement.

In the case of spasticity, it is theorized that there is some miscommunication between the signals generated by these organs and how they are interpreted in the brain and spinal cord. Spasticity is a common symptom of many different maladies, including but not limited to Cerebral Palsy, Multiple Sclerosis, and Stroke, all of which manifest as some level of damage in the cortex. It is characterized by unpredictable and uncontrollable muscle contractions, increased muscle tone, or a series of rapid contractions. For a patient diagnosed with spasticity, normal movement patterns will exceed the threshold for reflex activation, meaning that the stretch reflex will become active as if the limb were moving too fast or over extended. This hypersensitivity will result in hypertonicity in the affected muscles, causing disruption in motor control activities including gait, speech, and other movements.

A very clear explanation of this phenomenon is described by Jobin et al. (2000) as shown their graph (Figure 1.1). This graph shows the range of motion (Θ- and Θ+) on the X axis and a unit less velocity range on the Y axis and a theoretical plot of the activation threshold for patients with cerebral palsy and normal subjects.

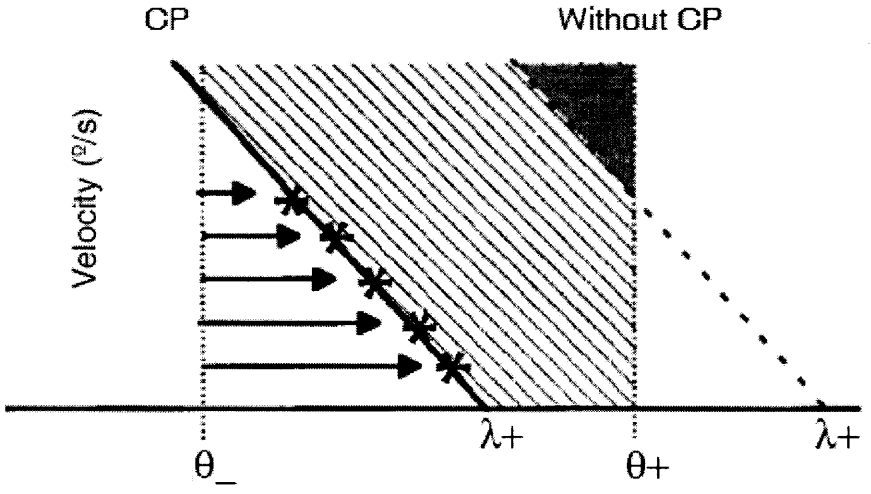

Figure 1.1 Stretch reflex activation curves for healthy subjects and patients with spasticity.
Source: Jobin, A., Levin, M., (2000) "Regulation of stretch reflex threshold in elbow flexors in children with cerebral palsy: a new measure of spasticity." *Developmental Medicine & Child Neurology*, 42: 531-540.

This graph shows how for a normal subject, the threshold hold to activate the stretch reflex is far outside the biomechanical range of motion at low speeds, and can only be achieved at very high speeds at the extreme range of motion. In a patient with cerebral palsy, this threshold for activation is within the normal range of motion of the joint at both high and low speeds.

When the centers that process incoming proprioceptive information do not function correctly, the stretch velocity and position are considered outside the threshold for safe movement, and therefore an efferent signal is sent to the corresponding gamma motor neurons of the antagonist muscle. Gamma motor neurons innervate the intrafusal fibers in the muscle and are unable to generate force. However, when they contract, they alter the threshold for activation of the reflexes governed by the muscle spindles, raising the gain of the system, thus increasing the probability of causing a contraction that opposes the direction of movement (Jobin et al 2000). To overcome this antagonist

contraction, the active muscle needs to generate more force to continue the movement. For this reason, attempting to move even slowly through a range of motion is met by a series of stops and starts uncontrolled by the subject. A simple movement that should be characterized by controlled, predictable muscle contractions instead a series of contractions opposing the movement, and a series of stronger contractions to overcome the opposition.

The action of antagonist activation is called co-contraction. While a small amount of co-contraction is normal in healthy subjects to help keep the limb and joint stable during movement, excessive co-contraction is a common concern for spastic patients. During co-contraction, both flexor and extensor muscles are generating torque about the joint axis of rotation, and to produce a movement one muscle must generate more torque than the other. For a normal person holding a 20 N weight out in front of their body, the biceps muscle contracts to create a moment vector exactly equal to the moment created by the weight and the triceps muscle becomes almost completely relaxed. This is the optimal arrangement since no extra forces are created. In the case of a joint undergoing co-contraction, to hold the same 20 N weight out in front of the body the biceps muscle not only has to create a great enough moment to overcome the moment due to the weight, but also has to overcome the moment that the involuntarily contracted triceps muscle creates. The energy expenditure for this pattern in even the simplest tasks is much greater and has a much higher degree of difficulty.

While it is relatively easy to identify spasticity in affected patients, there are many different diagnoses that describe the different forms, each specifically describing which limbs are affected and to what extent. According to the National Institutes on

Neurological Disorders and Stroke (2002), Cerebral Palsy is classified both by the number of limbs involved and also by the type of movement disorder involved. Quadriplegia affects both the upper and lower limbs, Diplegia affects only the lower limbs, hips or pelvis, Hemiplegia affects only one side of the body, Triplegia affects three limbs and Monoplegia only affects one limb. The extent of the affliction is very much based on where in the brain the overall damage has occurred. The motor cortex is essentially partitioned into many areas based on its functional role (planning movement, initiating movement, etc) and also what part of the body it controls. It is possible, as evidenced by the various combinations of limbs involved, to have very localized damage that affects only one limb, damage that is confined to one hemisphere of the brain affecting only one side of the body, or bilateral damage that affects both sides of the body.

As defined by Bax et al. (2005), the classifications of Cerebral Palsy based on movement disorders include Spastic, Athetoid, and Ataxic. Spastic patients typically have muscles that are tighter and stiffer than normal that have a high resistance to being stretched. In the case of Athetoid (or dyskenetic) Cerebral Palsy, controlling and coordinating movements becomes extremely difficult, characterized by constant motion by the patient and speech difficulties. The primary cause for Athetoid Cerebral Palsy is due to damage to the basal ganglia or the Cerebellum. The basal ganglia are a group of nuclei in the brain that connect to the thalamus, cerebral cortex, and the brainstem responsible for motor control, cognition, and learning. The last major form of Cerebral Palsy is called Ataxic. This form is caused by damage to the Cerebellum at the base of the brain, which is the control center for balance and coordination, also coordinating the

actions of different groups of muscles. It usually affects all four limbs and the trunk, characterized by lower than normal muscle tone. Patients with this form of the disease exhibit a variety of symptoms, including changes in gait patterns manifested as wider than normal stance and overall shakiness of the movement, since lower than normal muscle tone causes the patient to constantly adjust their balance in an exaggerated manner. The most significant symptom of Ataxic Cerebral Palsy is tremor. It most often happens when the patient attempts voluntary movements, with the tremor becoming more severe as the limb approaches the target.

There are various treatments currently used to alleviate spasticity, each with its own benefits and drawbacks. One such treatment is to administer drugs either orally or intrathecally. Typically, the drugs are Gamma Aminobutyric Acid (GABA) agonists that amplify the inhibitory effects of the neurotransmitter GABA. GABA is a class of neurotransmitter that is responsible for the inhibition of a nerve signal (action potential) from transmitting from one neuron to the next. GABA receptors are directly coupled to chloride channels and also trigger second messenger systems that, when the neurotransmitter binds to the receptor, it triggers the opening of a chloride channels in the post synaptic neuron. Since chloride has a very negative equilibrium potential, increasing the cells conductance to chloride will move the overall voltage potential of the cell further from threshold, making it less likely to transmit the incoming action potential. When a drug binds to a GABA receptor, and the neurotransmitter is present, the ligand gated chloride channel remains open longer, allowing for a greater open time for the chloride channels causing more ions to rush in, lowering the overall voltage potential of the neuron and moving it further from the firing threshold. Ideally, the

hypersensitive/over firing neurons will be "calmed" by the presence of these types of drugs, allowing for more controlled voluntary movements.

These drugs that affect GABA receptors and are administered to spastic patients are typically benzodiazepines that act on $GABA_A$ receptors. In a study performed by Hevers et al. (1998), it was shown that benzodiazepines show a very high affinity for $GABA_A$ receptors and bind unselectively. Once bound, the benzodiazepine locks the $GABA_A$ receptor into a conformation where the neurotransmitter GABA has much higher affinity for the $GABA_A$ receptor, increasing the frequency of opening of the associated chloride ion channel and hyperpolarizing the neuron. This increases the inhibitory effect of the available GABA leading to sedation and anxiolytic effects.

Different benzodiazepines can have different affinities for $GABA_A$ receptors made up of different collection of subunits. McLean et al (1988) showed that the anticonvulsant/spastic properties of benzodiazepines may also be due to binding to voltage-dependent sodium channels rather than benzodiazepine receptors. Sustained repetitive firing seems to be limited by benzodiazepines effect of slowing recovery of sodium channels from inactivation.

Baclofen is a popular drug that has a similar effect on the central nervous system as benzodiazepines. It was found by Leo et al (1992) that it can be administered orally or intrathecally, it is a derivative of GABA and is an agonist to specific $GABA_B$ receptors which activate a G-protein coupled mechanism to increase transmembrane potassium conductance. For these purposes, Baclofen is designed to affect the spinal cord since it is the connection between the brain and the body's periphery. The spinal cord plays a role as a reflex system that functions as a feedback loop and Baclofen is thought to work on

this reflex circuit's Renshaw cells. Renshaw cells are inhibitory interneurons located in the gray matter that monitor the excitatory action of the alpha motor neurons and also to send an inhibitory axon to synapse with that alpha motor neuron. For a small population of patients, a physician may implant an intrathecal Baclofen pump, which administers the drug directly into the spine. The dose of intrathecal Baclofen necessary to slow down the reflex circuit is variable but is generally much smaller than the oral dose. This is usually reserved for patients that cannot control their spasticity or convulsions by the normal oral doses.

The use of Botox (botulinum) injections is also a popular mode of management for spasticity. It is essentially designed paralyze the lower motor neurons in the muscles, blocking the signal transduction from the neuron to the muscle, thus lowering the amount of involuntary movement and the power of muscular contractions as a whole. By injecting botulinum A toxin into the muscle, it prevents the release of acetylcholine at the neuromuscular junction, and stays effective for a period of four to six months (Filippi et al. 1993). The main problem with this therapy is that it is difficult to pinpoint the exact location that is needed to be inhibited, so often times other supplementary muscles will be affected by the injections, and the amount of toxin that is needed to partially paralyze a muscle is so small that even a small overdose will cause total muscle paralysis. Alcohol and phenol injections are also used to decrease the extent and frequency of muscle contractions in affected limbs by paralyzing the motor neuron.

CHAPTER 2

ASSESSMENT OF SPASTIC CEREBRAL PALSY

2.1 Problem Statement

The problem with various treatments of spasticity is that there is a very poor level of standardized evaluation criteria for measuring the symptom, thus making treatment assessments and progress very difficult to quantify and taking away from their strength and significance. Typically, a trained therapist will use one or more measurement techniques to evaluate the extent and severity of spasticity in the patient. These tests usually involve the therapist moving an affected limb in a specific manner (speed, range of motion) and essentially judging the patient on a vague scale that uses only a subjective evaluation of resistance to movement and range of motion.

Figure 2.1 Ashworth test on elbow joint.
Source:http://www.kompetenznetz-schlaganfall.de/uploads/pics/Ashworth-Skala.jpg, accessed Jan 2, 2008

The problem with this approach is that historically, different therapists will have different scores for the same patient and the ambiguity of the scaling system can justify both of the outcome measures. As the therapist moves the limb through a range of

motion they are essentially feeling for how the torque generated by the agonist and antagonist muscles of that limb vary with speed and position, all characterized by the stiffness and contractions that the therapist may or may not feel. Hence, the lack of a reliable, non-subjective measure to evaluate changes in spasticity after various treatments makes the apparent effectiveness of the treatments less reliable.

It has been shown however, that there is some intra-rater reliability in these subjective measures; while different therapists may score the same patient differently, a single experienced therapist has a relatively good consistency when scoring the same patient over and over again, but typically only on the upper extremities. Since there are numerous therapists currently trained on how to do this test, intra rater repeatability is not a good enough reason to use these tests with great faith. Since the therapist is essentially judging joint torques, contraction frequency, and locations of these contractions with respect to position and angular velocity throughout the range of motion, it is worthwhile to employ an instrumented system that can actually measure all of these parameters accurately and with a high level of repeatability as the test is taking place. While there still may be a certain need for training to use the piece of equipment, all the measurements taken will no longer have to be evaluated for human error.

The use of EMG observation has grown in popularity when characterizing spastic contractions. The main reason it is used is to pinpoint where in the movement the muscle first contracts. It has also been a valuable tool in distinguishing between spasticity and contracture at the extremes of a limb's range of movement. When a therapist moves the limb they may feel more resistance toward the end of the range of movement and they have no way of distinguishing whether or not this is because the muscle is actually

contracting (active resistance to movement) or the intrinsic properties of the muscle have changed and that position is really the furthest point that the limb can physically move to (passive resistance to movement). If the therapist thinks that the muscle is contracting but the end of the ROM has been reached it may lead to a higher Ashworth score, and if the muscle is actually contracting but the therapist thinks that the end of the ROM has been reached they may assign a lower Ashworth score. By attaching surface electrodes over the muscles the therapist can see whether or not the resistance that they feel at the end of the range of movement is the contraction of the muscle or contracture of the tissues and an overall decrease in the range of movement of the limb.

The spastic form of CP is characterized by increased muscle tone, a hyperactive stretch reflex, exaggerated deep tendon reflexes, and sometimes clonus. Clonus is the term used to describe a series of involuntary high frequency muscle contractions in response to the lengthening of a muscle. Spasticity can be characterized by the inability to shift the dynamic stretch reflex curve beyond the biomechanical range of the joint. These plots shown in Figure 2.2 made my Jobin et al (2000) show the threshold range for healthy subjects (top) and the threshold range for subjects diagnosed with spastic cerebral palsy. It is clear that the threshold for reflex activation for normal subjects is not located in the biomechanical range, indicated by the vertical lines, whereas the patients have a threshold within the biomechanical range.

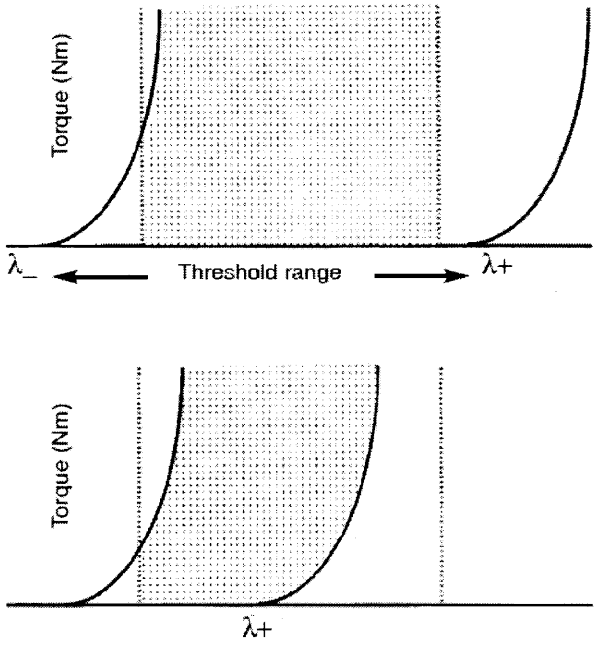

Figure 2.2 Stretch reflex threshold activation curves for healthy subjects (top) and patients with spasticity (bottom).
Source: Jobin, A., Levin, M., (2000) "Regulation of stretch reflex threshold in elbow flexors in children with cerebral palsy: a new measure of spasticity." *Developmental Medicine & Child Neurology*, 42: 531-540.

If the threshold is fixed at a point within the angular range of the joint, stretching the muscle beyond this point will cause spastic resistance. Since any stretch beyond the threshold angle will cause excitation, contractures commonly develop at this threshold point if the antagonist muscles are not sufficiently strong to oppose the spastic contraction (Jobin et al 2000). The location towards the end of the range of motion where to muscle begins to contract (resist movement) regardless of velocity is typically a good predictor of contracture. The patient will be less likely to extend the joint to the end of the range of motion since spastic contractions cause discomfort, therefore this portion of the biomechanical range will not be used. Over time, due to a smaller range of motion, the muscle will shorten and eventually change its composition to connective tissue.

Stretch reflex excitability may be influenced by a number of factors, including emotional stress and muscle fatigue. Simultaneous activation of the extensor and the flexor muscles was consistently shown in the study by Pisano et al (2000), especially during the fastest stretches, called reciprocal excitation. The static stretch reflex threshold is affected by both central and peripheral inputs but may be less influenced by changes in the mechanical properties of motor units.

2.2 Non-Objective Measures Used for Diagnosis

Bryan Ashworth (1964) created a five point scale that allowed for clinicians to grade the amount of resistance that they felt during passive movement.

Table 2.1 The Original Ashworth Scale

Ashworth Score	Description
0	No increase in tone
1	Slight increase in tone giving a catch when the limb is moved in flexion or extension
2	More marked increase in tone but limb easily flexed
3	Considerable increase in tone, passive movement difficult
4	Limb rigid in flexion or extension

Source: Ashworth, B. (1964). "Preliminary trial of carisoprodol in multiple sclerosis." Practitioner; 192:540-2

The Ashworth scale is commonly used to track changes in the passive resistance to stretch in patients during rehabilitation as a quantifier of recovery. The tone that is graded is defined by two physiological mechanisms: the intrinsic properties of muscle, tendon, and connective tissue and the active contraction of the muscle. Blackburn et al

(2002) states that typically, there is reasonable repeatability of measures between raters (interrater reliability) with the elbow joint, and poorer reliability with testing on the lower limb joints. Also, better standardization of testing procedure may lead to greater reliability, since testing procedures are not always described in detail.

Another study by Brashear et al (2002) was used to examine the validity of the scale on just the upper extremities. Each rater assessed each subject twice and an overall comparison was made between the raters' score on the same subject, and on the individual rater's score between both trials with the same subject. The joints examined were the elbow, wrist, fingers, and thumb. The study found that the Ashworth Scale has good intra and interrater reliability when used by trained medical professionals to rate excessive tone and functional impairment in patients with upper limb spasticity after stroke. This study may indicate that the Ashworth Scale has some validity in a limited sense but still should not be used with impunity.

In 1987, Bohannan et al. developed different parameters to be used for the same setup as the original Ashworth scale. By using a Modified Ashworth scale to asses spasticity in adults with cranial lesions, the testers were able to agree on 86.7% of the ratings, with a Kendall Tau correlation was .847 with $p<.001$. The testing procedures and the confidence was limited to just the elbow flexor muscle group, as this was the only muscle tested in this newly developed scale.

Table 2.2 The Modified Ashworth Scale.

Grade	Description
0	No increase in muscle tone
1	Slight Increase in muscle tone, manifested by a catch or by minimal resistance at the end of the range of motion (ROM) when the affected part(s) is moved in flexion or extension
1+	Slight increase in muscle tone, manifested by a catch, followed by a minimal resistance throughout the remainder (less than half) of the ROM.
2	More marked increase in muscle tone through most of the ROM, but affected part(s) easily moved
3	Considerable increase in muscle tone, passive movement difficult
4	Affected part(s) rigid in flexion or extension
9	Unable to test

Source: Bohannon, R.W., & Smith, M.B. (1987) "Interrater reliability of a modified Ashworth scale of muscle spasticity. Physical Therapy., 67: 206-207.

By adding a 1+ to the scale they essentially made it non linear and added another parameter for observation, the "catch," that has been a subject of examination and classification in various other studies.

Another test that is relatively popular with some validity in the assessment of spasticity is the Tardieu Scale. It was developed in 1954 as a preliminary spasticity assessment tool with the evaluation criteria as follows:

Table 2.3 The Tardieu Scale

Velocities used for measurement with the Tardieu Scale:	
V1	As slow as possible (slower than the natural drop of the limb segment under gravity)
V2	Speed of limb segment falling under gravity
V3	As fast as possible (faster than the rate of the natural drop of the limb segment under gravity)
Tardieu Scale-Score Criteria	
0	No resistance throughout the course of the passive movement
1	Slight resistance throughout the course of passive movement, no clear catch at a precise angle.
2	Clear catch at a precise angle, interrupting the passive movement, followed by release
3	Fatigable clonus (less than 10 seconds when maintaining the pressure) appearing at the precise angle.
4	Unfatigable clonus (more than 10 seconds when maintaining the pressure) appearing at a precise angle.
5	Joint is immovable

Source: Tardieu, G., Shentoub, S., & Delarue, R. (1954) "A la recherché d'une technique de measure de la spasticite." Revue Neurologie ;91:143-4.

In 1999, Boyd and Graham developed the Modified Tardieu Scale whose main contribution was to standardize the alignment and position of both the patient and the limb during the trials. There was a high reliability in these studies and the ability to detect changes following clinical trials for treatments were detected with greater accuracy than the Ashworth, Modified Ashworth, and the Tardieu Scales.

According to Patrick et al. (2006) the Tardieu Scale takes into account the velocity dependant nature of spasticity, and one of its parameters is seeing how tone changes at different angular velocities during testing. While using the Ashworth Scale, a practitioner may overestimate the level of passive tone at certain points in the ROM due to intrinsic changes in the muscle or tissue. As the muscle becomes hyper excitable at the extreme range of motion, eventually a contracture will develop and the excitable region will now become the furthermost boundary of motion. Many times when this occurs, a practitioner will mistakenly classify this as just a higher overall tone in muscle and assign a corresponding score. Since the Tardieu Scale utilizes the velocity dependant nature of the stretch reflex, it can much more easily differentiate between resistance due to spasticity and resistance due to physiological changes in the muscle. This shows that contractures, which are very common in spasticity cases, add another confounding factor into the assessment of spasticity when described with the Ashworth Scale. A main limitation in this assessment tool is that the practitioner is required to approximate the joint angle of muscle contraction onset during the actual test, which is extremely difficult to pinpoint in more severe cases of spasticity.

The tests performed by therapists are quick but imperfect ways to measure both the force of contraction of the joint and the location in the range of motion where it occurs. The therapist bases their diagnosis on the perceived magnitude of the torque that was required to move the arm through this range of motion, whether this applied torque increased or decreased as the angle changed, and the angle at which the onset of a higher applied torque was felt. The goal of the research for this thesis is to develop a device that can record all of the same information that a therapist uses to score the patient, but in a

very precise, instrumented manner, effectively eliminating the need for judgment and interpretation by the tester to diagnose a patient.

CHAPTER 3

IMPLEMENTATION OF INSTRUMENTED MEASURES

3.1 Previous Developments

Since subjective measures have been brought into question due to lack of repeatability and consistency, various labs have attempted to produce equipment that will essentially do the same assessment as the practitioner but with an actual numerical correlate to the severity of spasticity. Testers and therapists have created devices to be used in replacement of the Ashworth test, and have a set up that closely mimics the procedures of the test they aim to replace. This is beneficial since there is less of a learning curve for a therapist that might be employed to assist in the study.

A study by Allison et al. (1995) uses a setup that controls the angular velocity, acceleration, and displacement of the joint in question, and the subsequent EMG signal from the stretching muscles was recorded. They examined if there was some correlation between scores on the Modified Ashworth Scale and the angle at which the first reflexive EMG burst occurred during stretching. They found that subjects with higher MAS scores had higher resistance to angular displacement measures, which correlates to a small amount of angular displacement before a spastic EMG burst occurred. Also, they found that as the angular velocity is increased for various trials, the overall EMG activity is greater than in the slower trials, giving strength to the concept that spasticity is dependant on the angular velocity of the joint being tested.

Another study was developed by Pandyan et al. (2001) to develop a portable, non-invasive, simple and safe to use in a clinical setting device that will measure the

resistance to passive movement of the elbow joint. The system consisted of a one degree of freedom force transducer and an electrogoniometer that measured the applied force and the range of movement. The point of application of the force with respect to the elbow joint was not standardized and the moments were not calculated. The movement pattern is described as the humerus abducted to 90 degrees, then fully flexed and rapidly extended within a pain free range of movement. It differs from normal testing procedures in that the Ashworth test does not rapidly move the arm through the range of movement. The subjects recently had a unilateral stroke, the test was performed by one assessor, and all of subjects (48) have MAS scores ranging from 0 to 1+. Although the instrumentation had the potential to mimic the testing procedures of the Ashworth Test, it was hard to see correlations between different resistances with different scores, most likely since the Ashworth scale loses much of its distinguishing power at low scores with negligible resistance to movement. It was shown that the associations between the Ashworth scores and the resistance to passive movement for scores 0 and 1 were poor, but the measurement system was good at quantifying the angle of the "catch" and describing other diagnostic phenomenon such as the clasp knife reflex.

As more specifications were added to the Ashworth test, it was argued by Damiano et al. (2002) that the validity of the test may have decreased. The main reason for adding these extra scores into the original Ashworth scale is due to the fact that many of the outcomes of the test tend to be clustered around the mid range. Also, it measures passive resistance to motion that may be influenced by more than just a heightened stretch response (structural changes to the tissues, etc). The study performed by this group used an isokinetic dynamometer (measures torque and holds rotational speed

constant) to quantify resistance to passive stretch and surface EMG was used to verify if a stretch response occurred and at which angle for the wrist joint. The dynamometer was used to move the limb at three preset velocities while resistive torque and EMG data were measured. It was shown that the magnitude of resistance in patients with identifiable stretch responses can reach much higher levels than typically seen in those without stretch responses, especially at higher velocities.

It was argued that in the absence of EMG verification, evaluating patients at different velocities may help to distinguish passive stiffness alone from reflex stiffness, but the Ashworth scale only uses one speed. This realization strengthens the resolve for developing instrumented devices that more accurately describe what is happening during the movement, or clinical scales with variable speeds (Tardieu scale) may be more useful, but still does not have much practicality as of yet.

All of these attempts to develop a good set of parameters to create instrumented measures to accurately describe joint mechanics have been met with a varying degree of impracticality following their development. They have all been somewhat successful in identifying various biomechanical aspects of spasticity but most are in a limited scope and could not be easily implemented in a clinical setting. Many of the setups use a rotary torque motor that moves the limb through its range of motion. This can be very dangerous if used on a patient that has lost an amount of a range of motion and the torque motor is not programmed correctly, causing the limb to move past its biomechanical range, thus injuring the patient. In the case of a patient with very severe spasticity, the device may also move the limb at speed that causes constant muscle contraction, which has the potential do cause soft tissue damage and pain for the patient. Also, the

implementation and adjustment of such a potentially dangerous device will take some amount of training, and is not likely something that a therapist would risk using for fear of liability.

3.2 Equipment and Software Overview

The first piece of equipment to be used to describe the joint mechanics of subjects is a six degree of freedom force sensor. Made by Assurance Technologies Inc (ATI), the force sensor measures forces in the X (perpendicular to wire attachment), Y (parallel to wire attachment), and Z (direction normal to the surface of the force plate) directions and the torques measuring the forces of rotation about all these axes. The force sensor reads into a mux box, then into the controller where the signals are integrated and filtered. Then the data is sent to the computer by way of an RS232 serial connection with a null modem adapter. The serial port was set at a baud rate of 38.4 kilobits per second, which was manually changed from the default rate of the force sensor. This was done by opening the system controller and changing the switch configuration for the highest baud rate port setting as described by the instruction manual, increasing the baud rate from 9.6 kilobits per second. The port was set to read eight databits, with one stop bit, no parity, and the flow control was set to software. Also, the buffer sizes were set to be very large (100000 bytes) to allow for all the data from each trial to come in and be read at a later time.

When using the force sensor without its proprietary software, command strings are required to be sent to the controller to set the data transfer and acquisition properties. A command was sent to bias (zero) the sensor, but this was only done on the first trial since re-biasing the sensor for every trial causes an inconsistency in baseline magnitude

between trials. This can also be done by opening the proprietary software controller and clicking the bias tab on the user interface and the bias will carry over to MATLAB program until the controller is reset. Then another command was sent to initialize the controller to start reading data from the strain gages. Data streamed from the sensor to the buffer for the set amount of time for each trial. The data was communicated to the computer in ASCII format, with each record (one reading for each degree of freedom plus an error flag) being 45 bits long. The sensor sampling frequency defaulted to about 2400 bits per second, so each full record was recorded at about 100 samples per second. Another command was then sent to the force sensor controller to stop the data streaming. The data was then read from the serial port buffer into MATLAB as an ASCII string in a single column. It was then sorted for just the numbers, since the data contained commas and echoed back character commands. It was then converted into characters and transposed. Then, the data was broken down into its individual vectors by column. Now the data was in an easily usable format.

The Flock of Birds (Ascension Technologies) data also made use of an RS232 serial connection to the computer and also used MATLAB to communicate. The port settings were configured and setup commands were written and sent to the sensor controller to dictate the data streaming properties including angles read and rate of data transfer (100 samples per second). A command was then sent to stream the data into the buffer and then the data was read and imported into MATLAB where it was already separated into its angular components. All of the programming code to run the equipment is included in Appendix A.

All the data from both pieces of equipment were processed in the MATLAB workspace. The data was filtered with a second order low pass Butterworth filter with a cutoff frequency of about 10 hertz, since sampling rate was never the exact same from trial to trial a close approximation was used. Then, the filtered angle data was differentiated to find angular velocity, filtered again, then differentiated and filtered once more to find acceleration. The programming code used to process the data is included in Appendix B.

While this device has a large amount of potential when it comes to both normalizing and quantifying commonly used, imperfect tests performed by therapists, it also has uses that may help it describe the basic mechanics of the muscles at a joint in a much more informal way. Since it allows for movement and forces in flexion and extension, it can be used to push or pull the limb through its range of motion while giving accurate readings of force while at the same time it records positional information with angle, angular velocity, and acceleration. This can be particularly useful when attempting to describe the kinematics of joints under certain conditions, since many of the variables (joint torque, stiffness, etc) can be solved for by knowing the angular velocity and acceleration, as well as all the relevant anthropometric data for each subject. The kinematic equation is as follows: $M_{applied}=I*\alpha+\beta*\omega+k(\Delta\theta)+m*g*l*\sin(\theta)$, where I is the moment of inertia, β is the damping, k is the stiffness, and the last term is the moment due to gravity.

3.3 Calibration

The force sensor was mounted on a rigid, non elastic Velcro strap and has a rigid metal loop directly attached to the mounting plate on the opposite surface. By having the force sensor mounted in this orientation it allows for both pushing and pulling motions to have accurate measures during the experimentation, since it is simply putting the surface of the sensor under tension and compression. This setup differs from other studies (Pandayan et al 2001) in that it allows for the measurement of both forces in extension and flexion with an accurate degree of certainty. Since the force sensor records six degrees of freedom (Fx Fy Fz Tx Ty Tz) it allows for a complete picture of the force recorded by the sensor, but for this study only the Fx Fy and Fz vectors were needed. For this reason, during the programming of the instrument a command (CV 7) was sent that disabled the torque vectors since they were needless. Not only did this make the data processing in the end easier to sort, but also increased the overall frame rate of the system since 21 bits from each full record were passed over, six from each torque vector and an extra three for the ASCII character for comma. Then another command was passed to the controller to enable it to communicate fast (CF 1). On the default setup, the controller periodically checks the sensor conditions and does a sensor average, but this slows down the overall read rate and transmission, so these tasks were eliminated with the CF 1 command. Under this condition, the frame rate can reach a maximum of 160 Hz, but is set to 100 Hz to allow similar data sets for the force sensor and the Flock of Birds.

The program created a total force vector by taking the root sum of the squares of the three force vectors. This vector allows the user some flexibility when conducting

experiments, since looking at just one force cannot show with certainty that the user is moving the subject with a force that is truly tangent to the arc of motion of the limb. Also, in experiments that are conducted where the subject is not moved in the plane of gravity, it is possible for solve for the movement force by examining the total force vector. Depending on the orientation of the experiment, a predictable amount of force will be required to support the limb throughout the movement (m*g*l) that can be subtracted out of the total force vector, leaving just the forces acting in the plane of movement.

3.3.1 Synchronization of Flock of Birds to Force Sensor

The data streams from the Force sensor by way of an RS232 serial connection at a maximum rate of approximately 160 Hz, which was reduced to 100 Hz (SF 100) to make it easier to correlate with the other equipment running at 100 Hz. All parameters are set and triggered in the MATLAB computing language, and the program is set to trigger both the force sensor and the Flock of Birds at approximately the same time, then throws out the first few records of data at about the same time right before the actual collection of data into the buffer occurs. This essentially syncs the two devices so that the time stamp on both angle and force data will be the same. The problem with this technique is that since the force sensor records at approximately, but not exactly, the rate of the Flock of Birds, by purging the unsynchronized data from the force sensor it frequently cuts off data mid record, giving a partial unusable data record. By searching for the position of this error in the 24 bit word (45 for the total word minus the 21 comprising the torque data) for the first record it is possible to eliminate the unusable data and approximate the

amount of time that has passed in the data before this occurs, then delete a proportional amount of data records off the beginning of the Flock of Birds data stream. This ensures that both the force and angular data are still synchronized and that the final variables are arranged in an easily manipulated matrix.

As proof that the two devices are synchronized, a tool was created to help verify this fact and also to help in the calibration process. The entire program was run once with the sensor biasing command running while the force sensor was held by the side of the casing, as to bias the signal to zero and truly have no force inputs coming into the sensor. Then, the biasing command was removed and a mass of 500 grams was placed on the surface of the force sensor (compression) for half the trial and suspended hanging from the Velcro strap (tension) for the second half, and their magnitudes (~50 counts) were recorded and verified to be equal and opposite in direction. To make sure the Flock of Birds and the force sensor were synchronized, the two devices were attached to opposite ends of a PVC tube and attached rigidly. Then the 500 gram mass was placed on the surface of the force sensor and securely fastened to the tightened Velcro strap so that when right side up the mass will be compressing the sensor and while upside down the mass will be pulling on the Velcro strap with the same force.

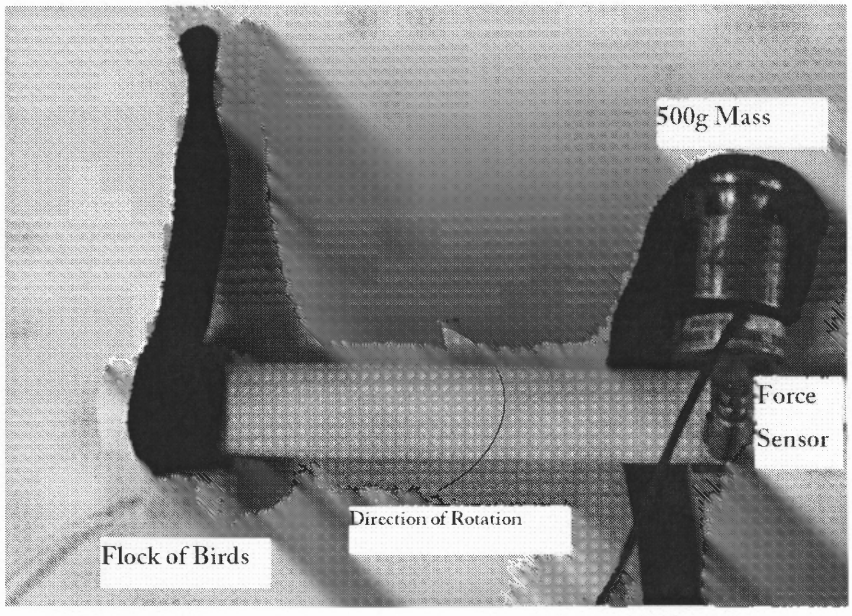

Figure 3.1 Calibration Setup 1

The tube was then rotated 180 degrees, then rotated back 180 degrees over and over for the full amount of trial time. It was shown that when the PVC pipe was horizontal, the greatest amount of normal force was exerted on the sensor and the angle equaled either positive or negative 90 degrees and they reached these values at close to the same time, with a slight lag in the angle measurement caused by a swing of the attached weight as its orientation approached vertical, causing some variability in the peaks of the force measurement. Furthermore, the force crossed the zero axis when the tube was held vertically and at this same time the angle was also recorded as zero, adding strength to the idea that these devices are in fact synchronized. The derivatives of both of these vectors were then taken and when plotted, crossed the zero axis at the same time, which would be expected if they were synchronized. The corresponding plots are as follows:

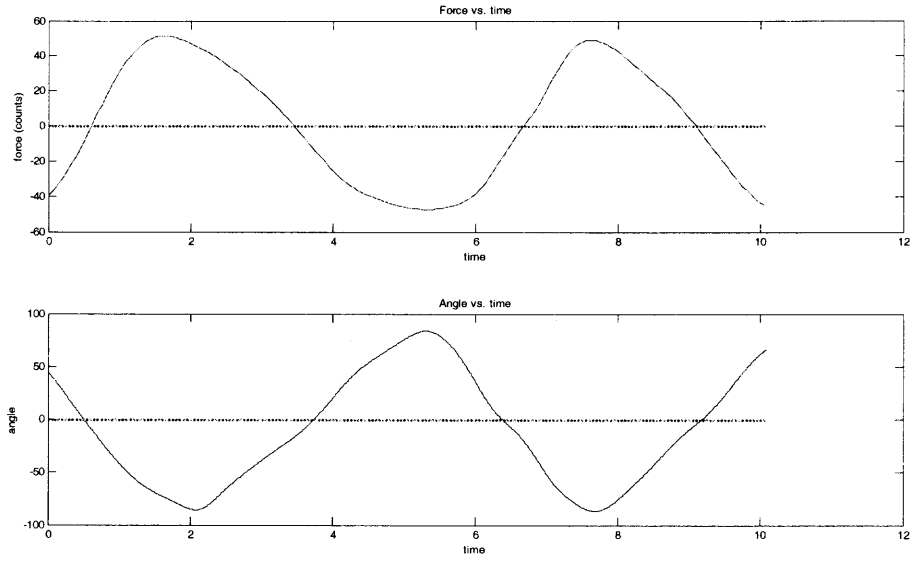

Figure 3.2 Calibration plot 1

3.3.2 Use of 2 Axis Force Measurement

During some of the experimental tasks, the weight of the limb of the subject will be constantly supported by the tester, so this will make full use of the three vectors of force that the sensor is capable of measuring. Ideally, if the metal ring is supporting a load attached to the nylon strap, the orientation of the sensor in space should not change the overall magnitude of the force vector being read by the sensor, only the axes that are reading the force will change in a predictable way according to the orientation of the weight with respect to gravity. To verify that this method was viable to measure a resultant force another method of calibration was used. The force sensor was mounted onto a rigid PVC tube about an inch below the end, and the Flock of Birds was mounted to rotate at a 90 degree angle from the Z axis of the force sensor. The 500 gram mass was secured tightly to the end of the PVC pipe about an inch away from the force sensor.

The PVC pipe was then pressed against a rigid surface as a pivot point. The program was run with the force sensor pointing straight up, so the Z axis was measuring the majority of the force, and about half way through the time the PVC pipe was rotated 90 degrees. At this point, the majority of the force was measured on the X axis.

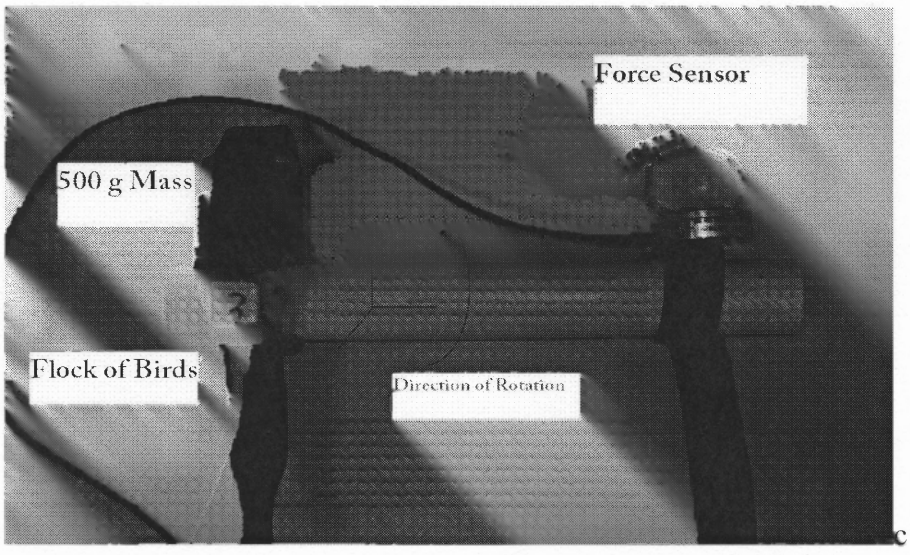

Figure 3.3 Calibration setup 2

The data was then plotted and at the time before the pivot, the Z axis read about 60 counts (force of 500 g mass and mass of tube) and after time of rotation the force in the X axis read the same force. The overall magnitude of the force vector (root sum of the squares of the forces) never changed throughout the entire trial time. This experiment shows that while the direction of the force relative to the axes of the sensor changes, the overall magnitude of resultant force vector doesn't change. The graph of this experiment (with the weight of the tube subtracted out) is plotted as follows.

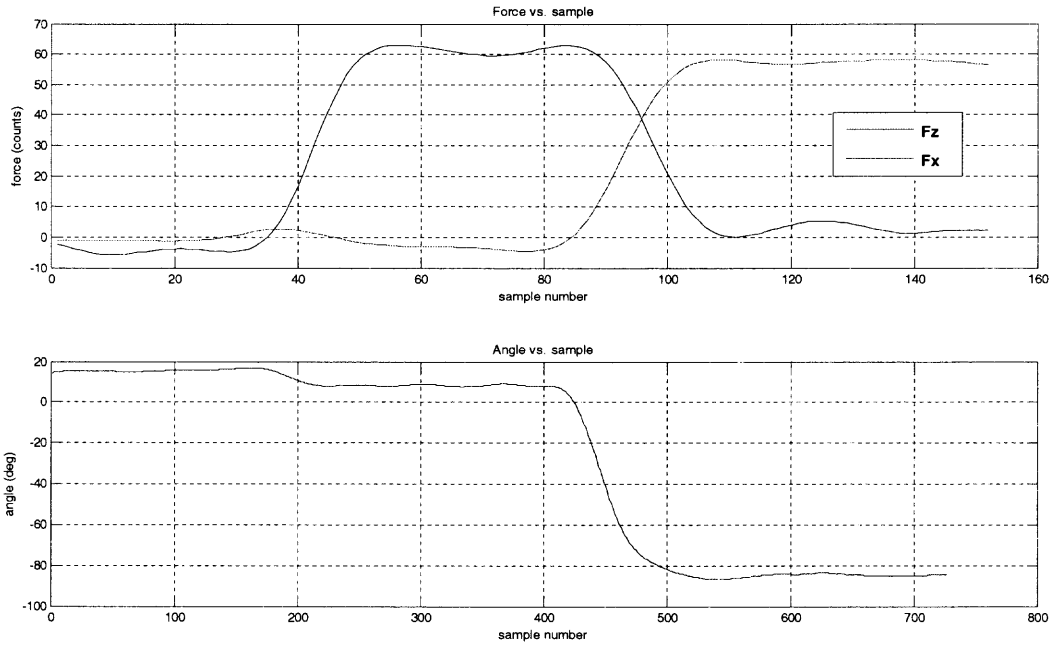

Figure 3.4 Calibration plots 2

This graph shows that when the angle is zero, the force is directed vertically (Z axis) and when it is rotated about 90 degrees the force in the Z axis goes to zero at the same time that the force in the X axis increases to the same level as the previous Z force.

CHAPTER 4

EXPERIMENTAL PROCEDURES

4.1 Subject pool

A subject pool of three healthy adults (two male, one female) was recruited for this study. The height (cm) and weight (kg) were recorded for each subject just prior to the testing procedures.

Table 4.1 Subject pool and Anthropometric data calculations.

Subject	Sex	Height (cm)	Mass (kg)	Shank length (cm)	Shank and foot length (cm)	Shank and foot mass (kg)	I ($kg*m^2$)
1	f	160	76.66	39.36	45.6	4.68	.883
2	m	187.96	82.55	46.24	53.57	5.04	1.311
3	m	170.2	74.84	41.87	48.51	4.57	.976

Using the Mass Moment of Inertia equation given in Biomechanics of Human Motion (Winter 2005), $I = m*p^2 + m*x^2$ where I is mass moment of inertia, m is mass of shank and foot, p is proximal radius of gyration of the shank and foot, and x is proximal distance to center of mass of the shank and foot. The moment of inertia for each subject was calculated and located in the last column of table 4.1. All the free body diagrams for each task are included with their description.

4.2 Experimental setup and Data Collection

4.2.1 Task One

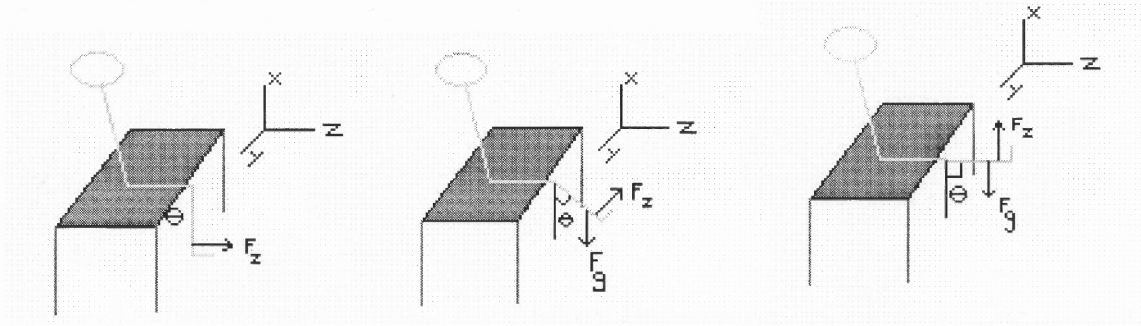

Figure 4.1 Free Body Diagrams of three phases of Task one

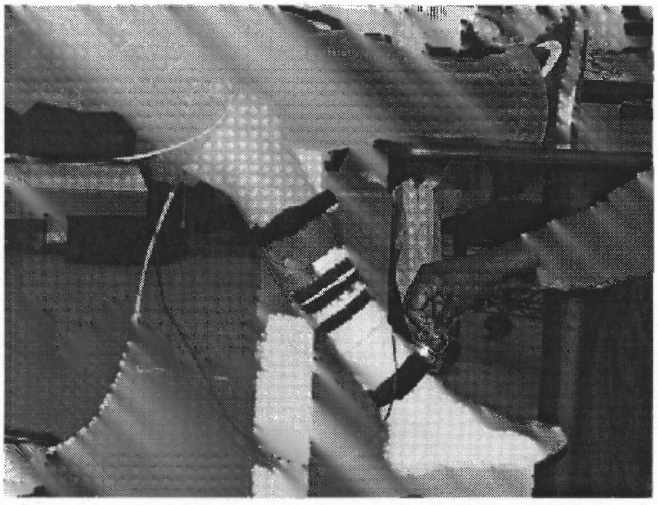

Figure 4.2 Attachment and orientation of instruments for Tasks one and Two

The first task used the instrumentation to measure a simple assessment of joint torque under passive movement conditions while being under the influence of the force of gravity as depicted in Figure 4.1. The subject was asked to sit on a table 72 centimeters tall with the lower leg hanging down off the table, swinging freely. Once it was

determined that the subject's lower leg can be extended and flexed throughout its comfortable range of motion with no interference from external objects, the devices were then attached to the lower limb.

First, the sensor for the Flock of Birds angle/position tracker was firmly attached on the front of the shin about three inches below the knee. It needed to be placed low enough so that it was out of the way of the extra skin that bunches at the knee during movement to avoid sensor movement relative to the knee, but not so far as to cause excessive movement of the wire that connects the sensor to the Flock of Birds box. Movement of the wire has been shown to cause noise in the data as it comes into the box, either due to electromagnetic interference caused by the wire interfering with the sensor signal, or by signal attenuation caused by the physical deformation of the wire as the information is traveling over it. The sensor was oriented so that as the knee angle changes it will be rotating about only the Y axis, as to minimize the amount of data processing since examining and filtering one degree of freedom of data is more efficient than creating a vector of rotation and doing the same. It was also shown that rotations about the other axes during the trials were less than the Flock of Birds' margin of error for the angle measurements. The force sensor was attached to the lower leg via a rigid nylon strap with Velcro attachments. It was tightly secured over the bony prominences in the lower leg (lateral and medial malleoluses) since this is the reference point used in anthropometric tables to signify the separation from the lower leg (shank) and the foot and could be easily calculated from the tables.

The subject was then asked to relax their lower leg completely and throughout the trials an assistant was present to keep the subject distracted from the test taking place.

The leg began freely hanging downward off the edge of the table and the metal ring attached to the force sensor was grasped only after data had started being recorded. The reason to grasp the ring after data had begun to be collected was to get quantifiable error reading that could be subtracted out of the data, since there is almost always some residual force present caused by the tightness of the straps. Then the leg was slowly pulled by the metal ring attached to the force sensor in a direction tangent to the arc of the motion of the leg. At the end of each trial a plot was created for a quick examination of the data to assure the measured values were accurate and without significant amounts of noise. The plots included the force data and angle data to see if the data read is correlated as it should be, and the angular velocity and acceleration of the leg to make sure that the leg was moved slowly for task one. A total of four trials were recorded since consistent data would indicate that there is minimal influence by the subject.

4.2.2 Task two

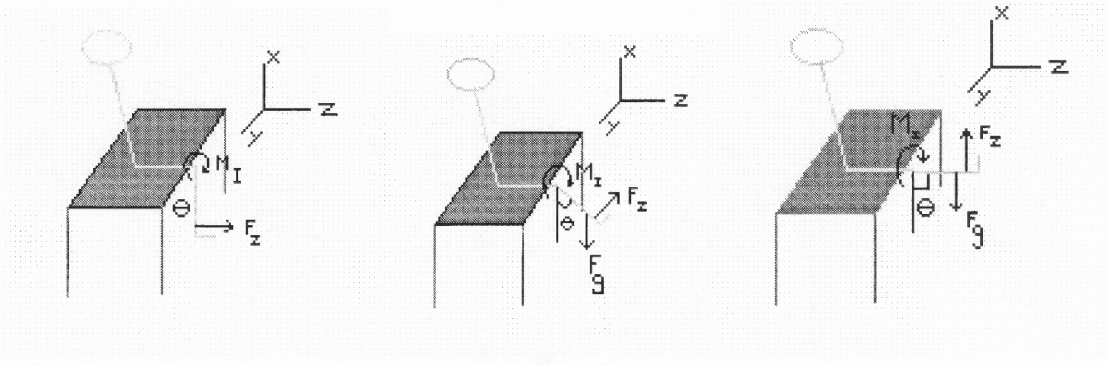

Figure 4.3 Free Body Diagram for Task two

The second task in this experiment was essentially the same procedure as the first task but the leg was moved much more rapidly as shown in Figure 4.3. It was pulled very quickly to full extension and the plots of the force, angle, angular velocity, and

acceleration were all created at the end of each trial to verify that there was minimal noise and the magnitudes of the values were predictable. Only trials with an angular velocity greater than 50 degrees per second were kept, as this signifies a high rate of angular change. A total of four trials were recorded for each subject in this task as well.

4.2.3 Task three

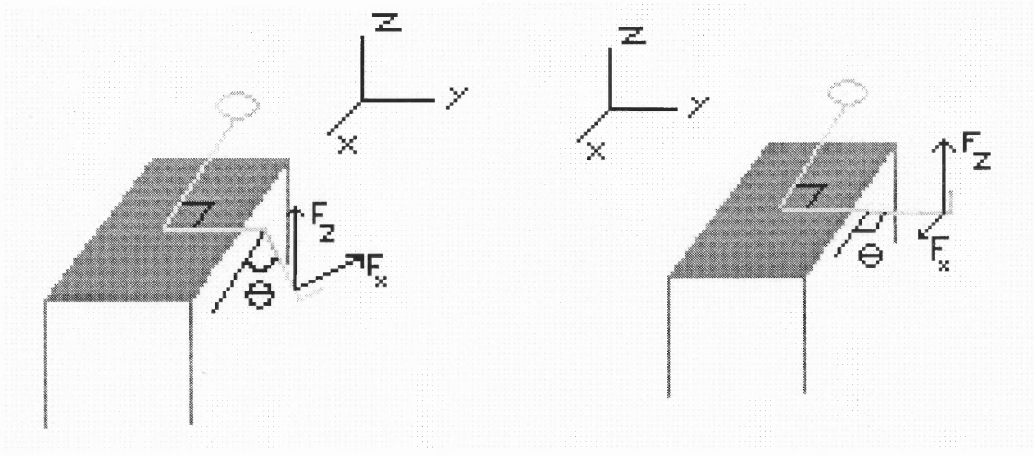

Figure 4.4 Free Body Diagram for Task three

Figure 4.5 Attachment and orientation of instruments for Tasks three and four

Next, a similar task was performed on the subject but with significant differences to the setup. In this setup, the subject laid on their side with their leg extended over the edge of the table as shown in Figures 4.4 and 4.5. This way, the lower leg does not pivot at the knee joint under the influence of gravity. Instead it was oriented perpendicular to the gravitational plane. Again the force transducer was attached very tightly to the lower leg at the bony prominences. The limb was then moved slowly through the range of motion, but in this instance another force was needed to support the leg as it hung off the edge of the table, otherwise the hip of the subject would rotate, causing the plane of movement of the lower leg to not align perpendicular to the field of gravity anymore. Since the force sensor measures forces in the X Y and Z planes, the force of the tester supporting the leg and the force to move the limb through the range of motion would be independent of each other. Again, the raw data was plotted immediately following each trial along with the total force vector to make sure the data was consistent before going on to the next trial. A total of four trials were recorded for each subject to show some consistency over the trials.

4.2.4 Task four

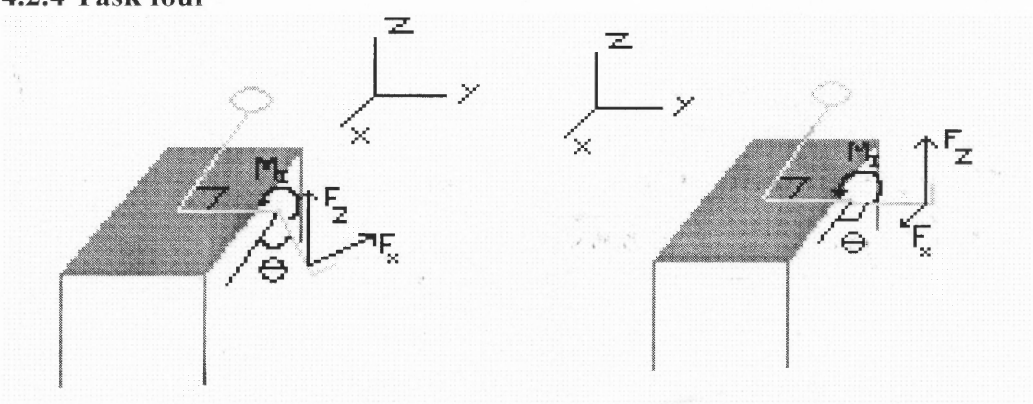

Figure 4.6 Free Body Diagram for Task four

The fourth task performed on the subject also called for the subject to be lying on their side with the force sensor attached around the ankle and the Flock of Birds just below the knee. Again, the tester pushed and pulled the leg of the subject while supporting it but in this trial it was moved very quickly as depicted in Figure 4.6. The leg was moved as quickly as possible until the tester felt that the end of the range of motion was being reached. A total of four trials were recorded to make sure the measures were consistent.

4.3 Data Processing.

4.3.1 Filtering Parameters and Vector Construction

The raw data was processed by creating coefficients in MATLAB by using the butter command that creates the parameters for a low pass Butterworth filter. The order was set to two, and the cutoff frequency was set to ten hertz, since it is highly unlikely that normal human movement can exceed this frequency, but still low enough so that most of the noise from movement artifacts, electromagnetic perturbations, and human error were minimized. Since the cutoff frequency entry into the butter function is actually the desired cutoff frequency divided by the sampling frequency, two different sets of coefficients were needed since the Flock of Birds and the Force Sensor run at slightly different sampling rates.

The raw force and angle data was then passed through the filtfilt command in MATLAB, which passes the data though the low pass Butterworth filter once, then passes the data back through a second time backwards, effectively doubling the filter

order. It is passed through backwards on the second filtering because a phase shift occurs, so by running it twice in opposite directions this phase shift is eliminated.

The angle data was then differentiated by a custom made derivative function in MATLAB that essentially took the difference in two consecutive data points and divided it by the difference in two points in a time vector. The time vector was created by taking the total number of samples and dividing it by the sampling rate of the Flock of Birds. This was done for all three vectors (pitch, roll, yaw) even though we are only interested in using one at this time, since in future experiments more than one rotation vector may be used. The new angular velocity data was then filtered again using the same parameters used to filter the raw angle data.

The angular velocity data was then differentiated again using the same custom derivative function and then filtered for all three axes, giving angular acceleration vectors. This data was to be used for calculating the moment of inertia for the limbs.

The force data collected in each trial was then converted to Newtons post-filtering by dividing the raw count force by 100 to obtain the mass in kilograms, then multiplied by 9.81 meters per second^2, the acceleration due to gravity, to get a final force in Newtons.

4.3.2 Anthropometric calculations.

The lower leg (shank) and foot masses and overall lengths were calculated using an Anthropometric table provided in David Winter's Biomechanics of Human Motion (2005). The length was used to find the approximate distance from the lateral condyle of the fibula to lateral malleolus that will be used as the moment arm when calculating the torques required to move the limb, and the forces are assumed to be tangent to the arc of

travel of the lower leg. The distance from the knee to the bony prominences was then converted to meters and was then multiplied by the force (Newtons) to give torque values for each subject and each trial in Newton meters.

The moments of inertia were calculated by using the equations given in chapter three of Winter's book (2005). For each subject, the mass, radius of gyration, and distance from the rotational joint to the center of mass were calculated using the anthropometric tables given. The moment of inertia is the rotational analog of mass when comparing rotational dynamics to basic dynamics, and is useful in predicting rotational torques that resist movement forces under dynamic conditions. For example, a very massive object or an object with most of its mass distributed far from the point of rotation will exert a high torque resisting external forces trying to rotate the system. The moment of inertia was useful in predicting the force value during tasks two and four where the limbs were moved at a fast rate making the angular accelerations greater than zero, thus adding a force ($I*\alpha$) to the kinematic equation.

From the anthropometric and the angle data, a plot was created of mass of the lower leg multiplied by gravitational acceleration, multiplied by length to the center of mass, multiplied by the $\sin(\theta)$, or $m*g*l*\sin(\theta)$. This term should accurately describe the passive torque on the limb due to gravity. For the tasks where the limbs were moved quickly, the velocity, acceleration, and the moment of inertia terms were factored into the equation.

CHAPTER 5

RESULTS

5.1 Data plots

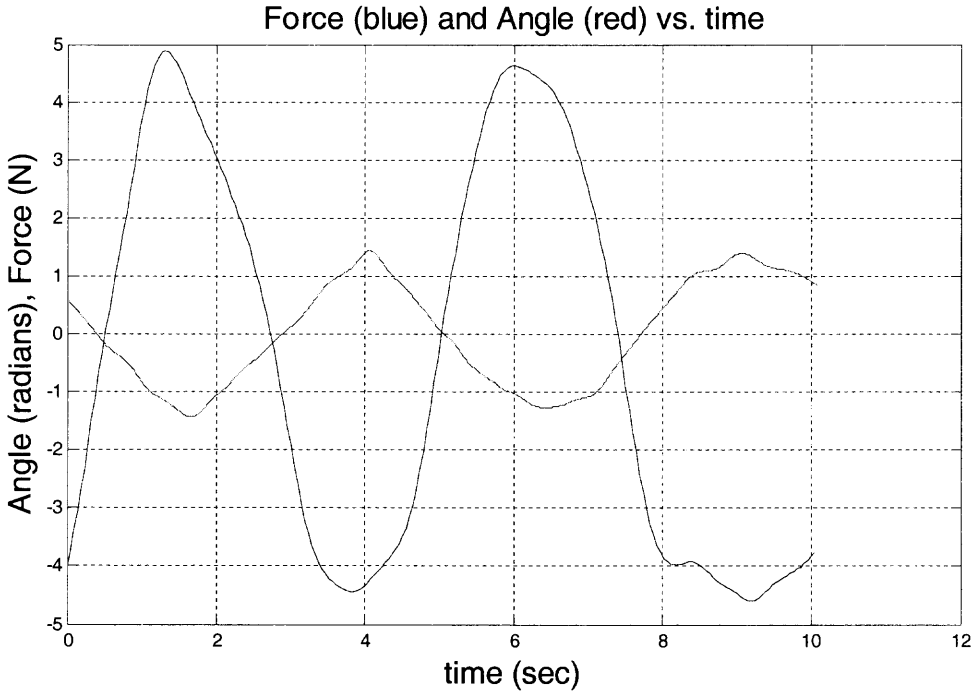

Figure 5.1 Calibration Plot of synchronized Force and Angle data

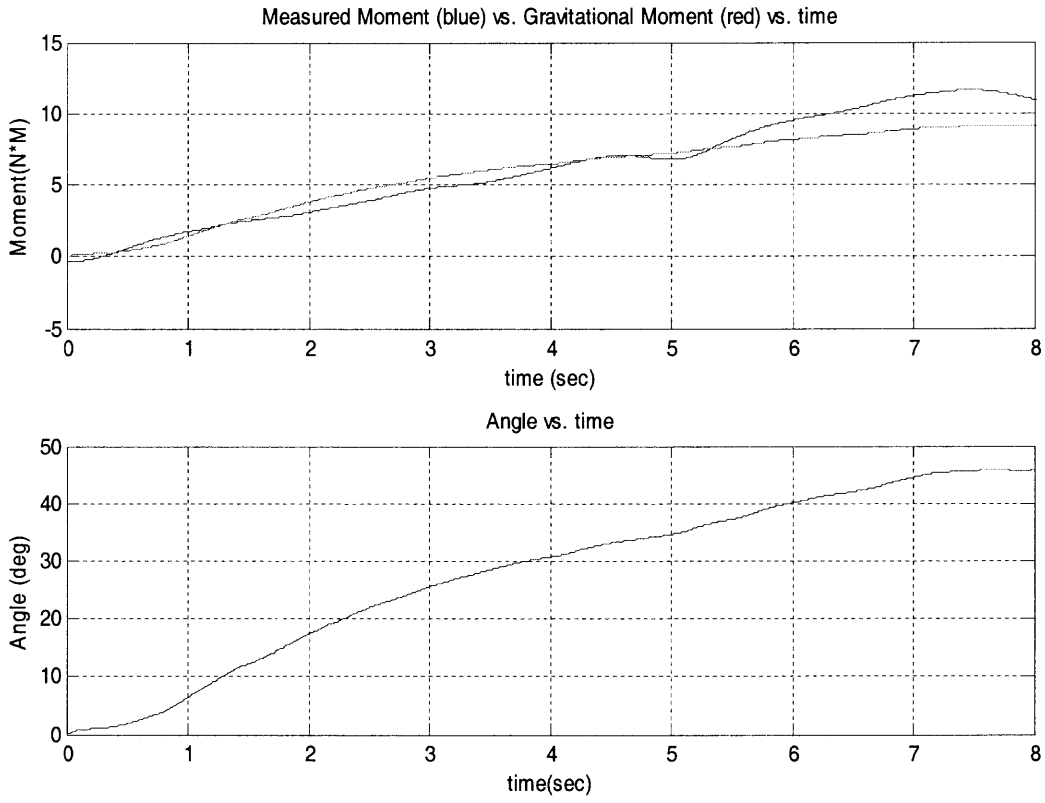

Figure 5.2 Measured moment (blue), gravitational moment (red), and angle plots for subject 1 Task 1

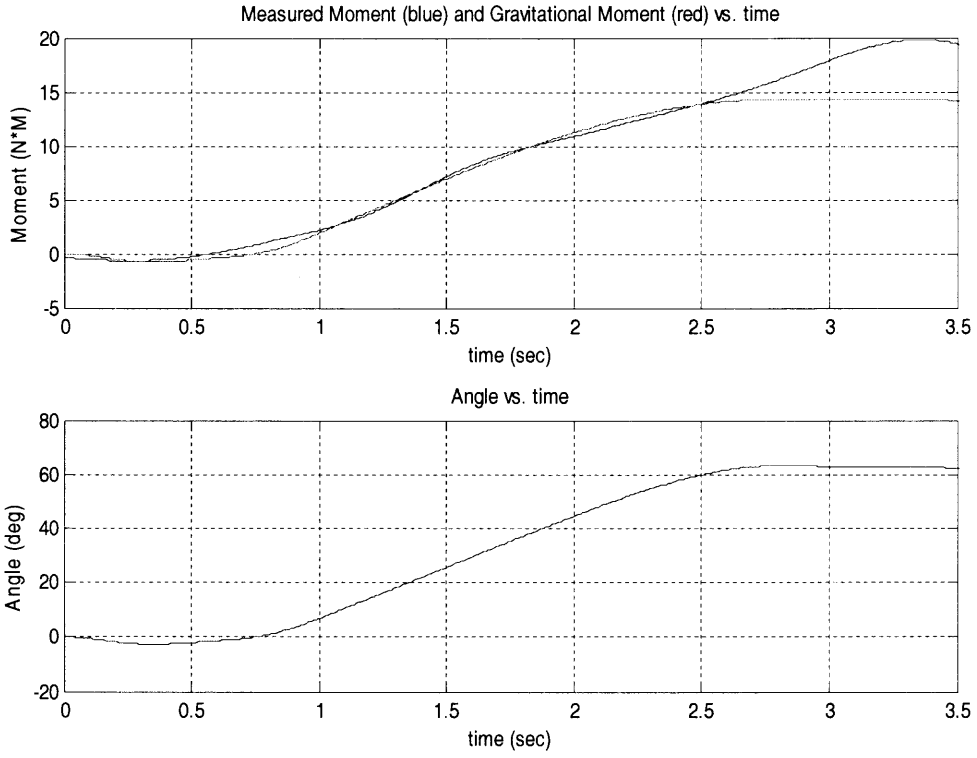

Figure 5.3 Measured moment (blue), gravitational moment (red), and angle plots for subject 2 Task 1

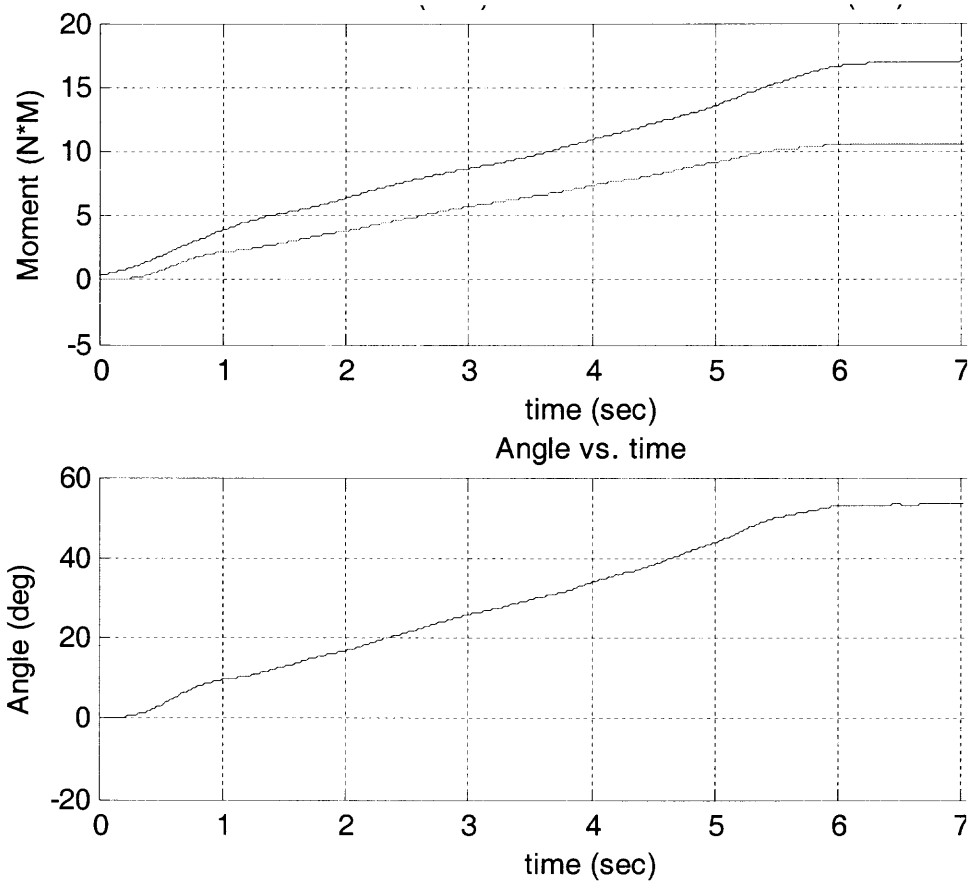

Figure 5.4 Measured moment (blue), gravitational moment (red), and angle plots for subject 3 Task 1

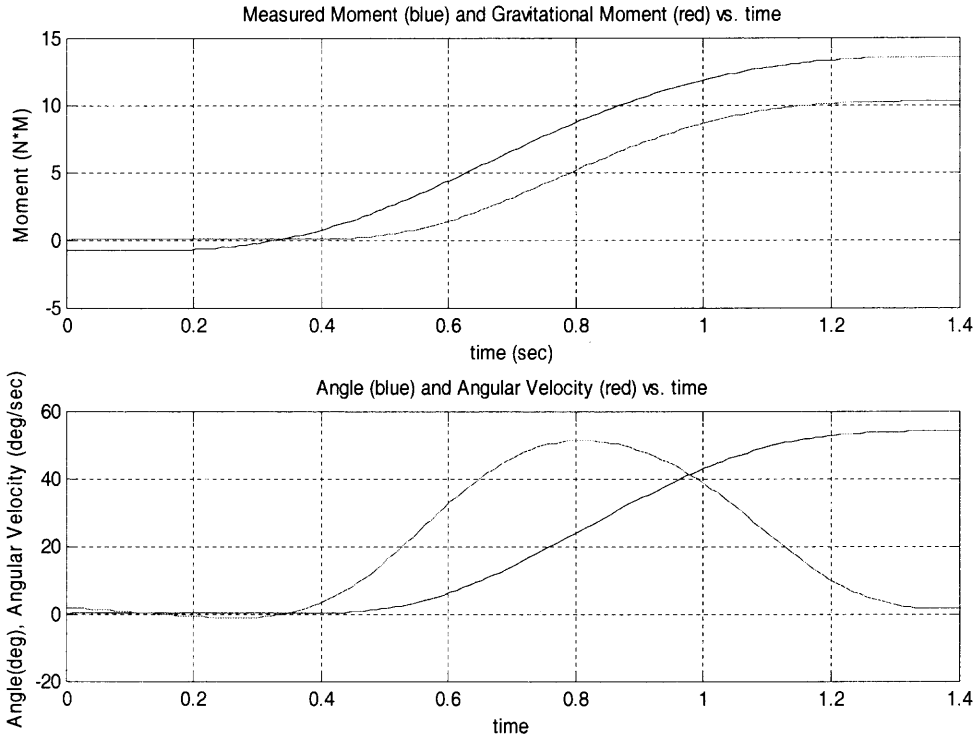

Figure 5.5 Measured moment (blue), gravitational moment(red), angle (blue) and angular velocity (red) plots for subject 1 Task 2

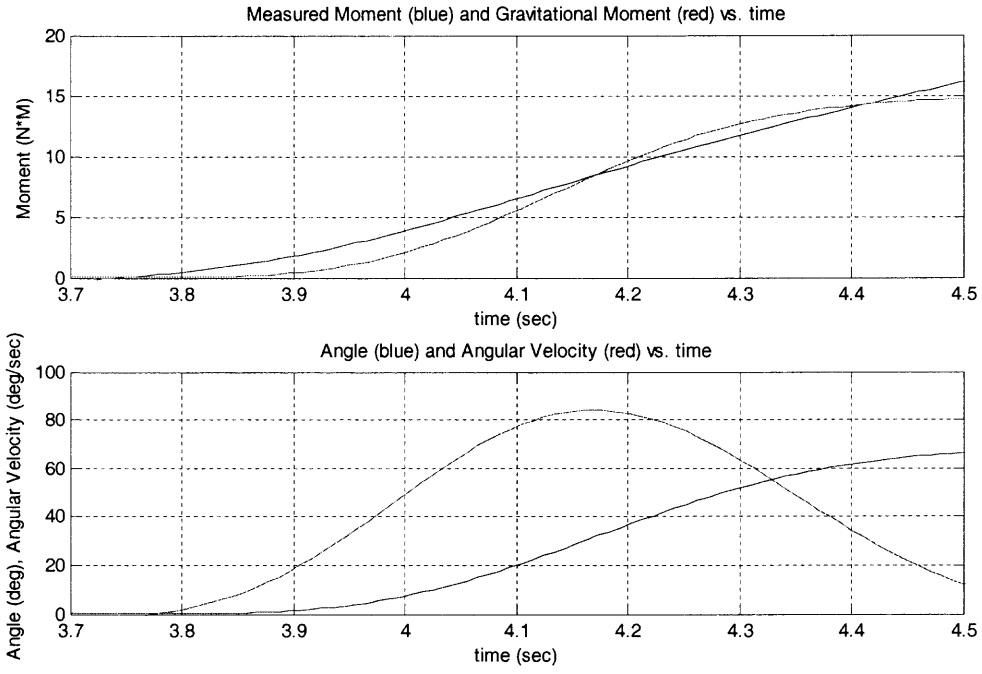

Figure 5.6 Measured moment (blue), gravitational moment (red), angle (blue) and angular velocity plots for subject 2 Task 2

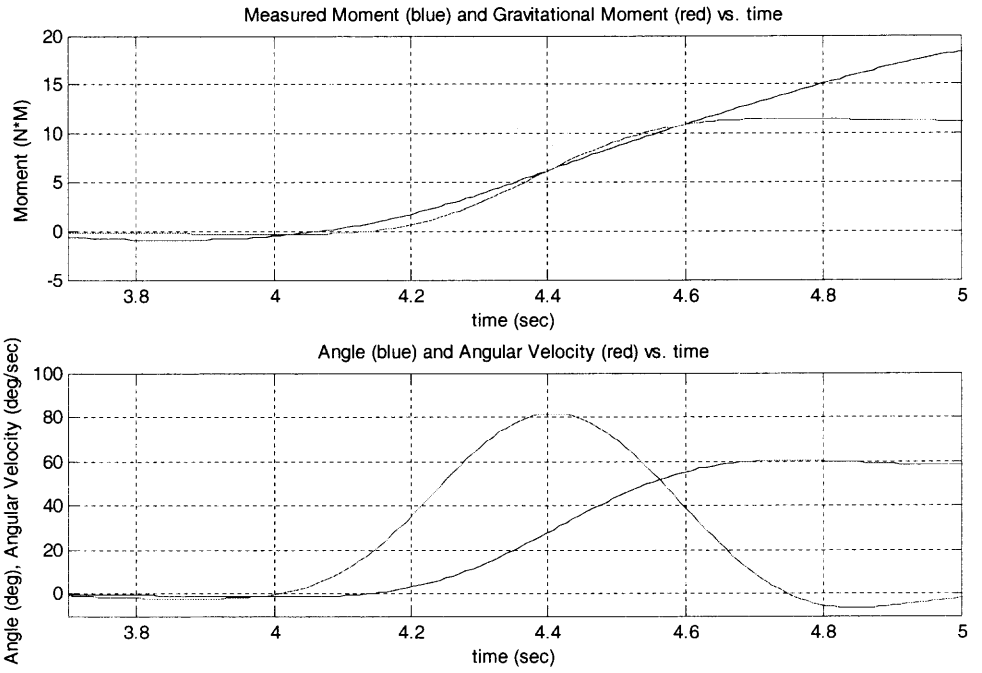

Figure 5.7 Measured moment, gravitational moment, angle and angular velocity plots for subject 3 Task 2

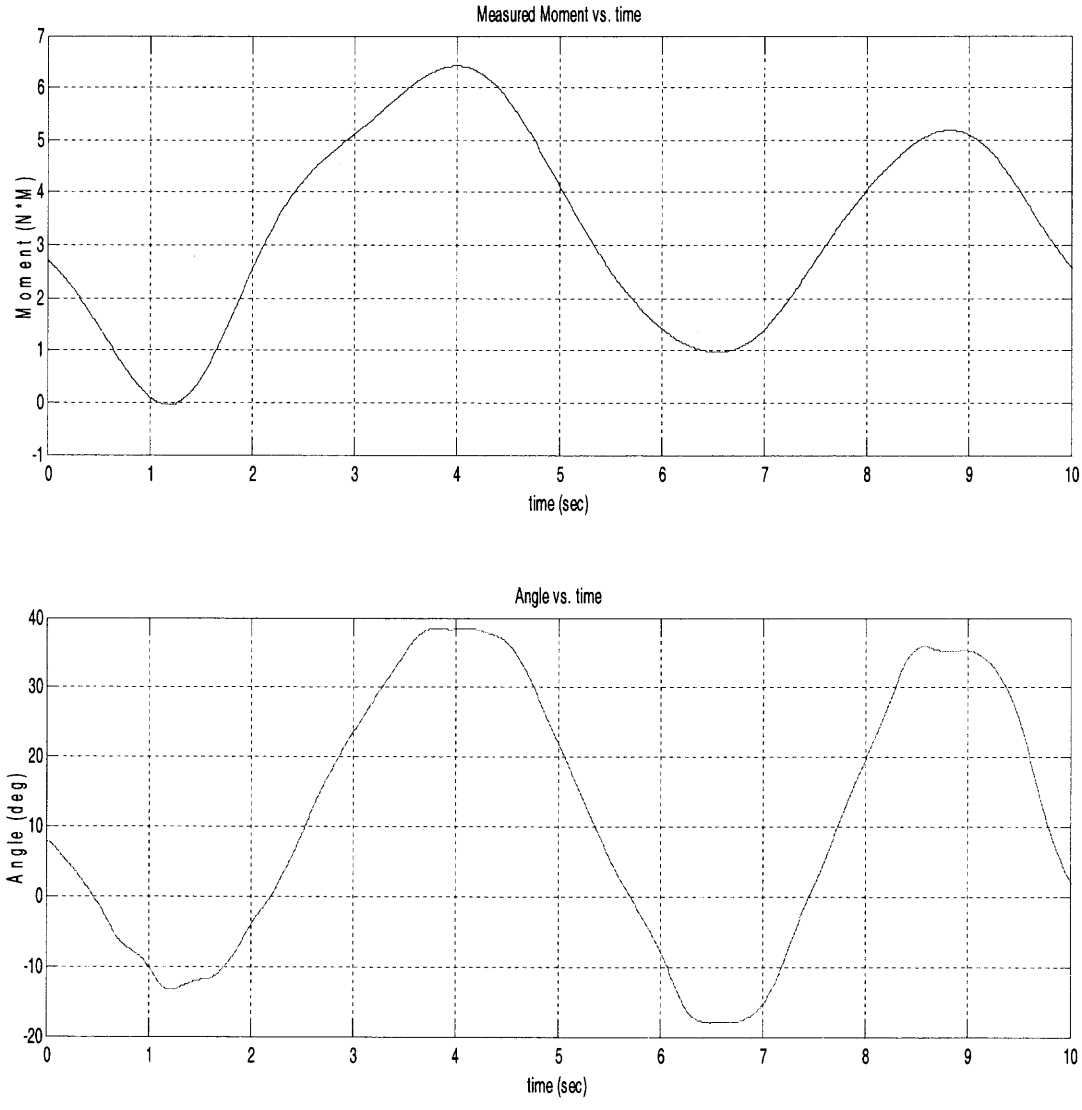

Figure 5.8 Measured moment and angle plots for subject 1 Task 3

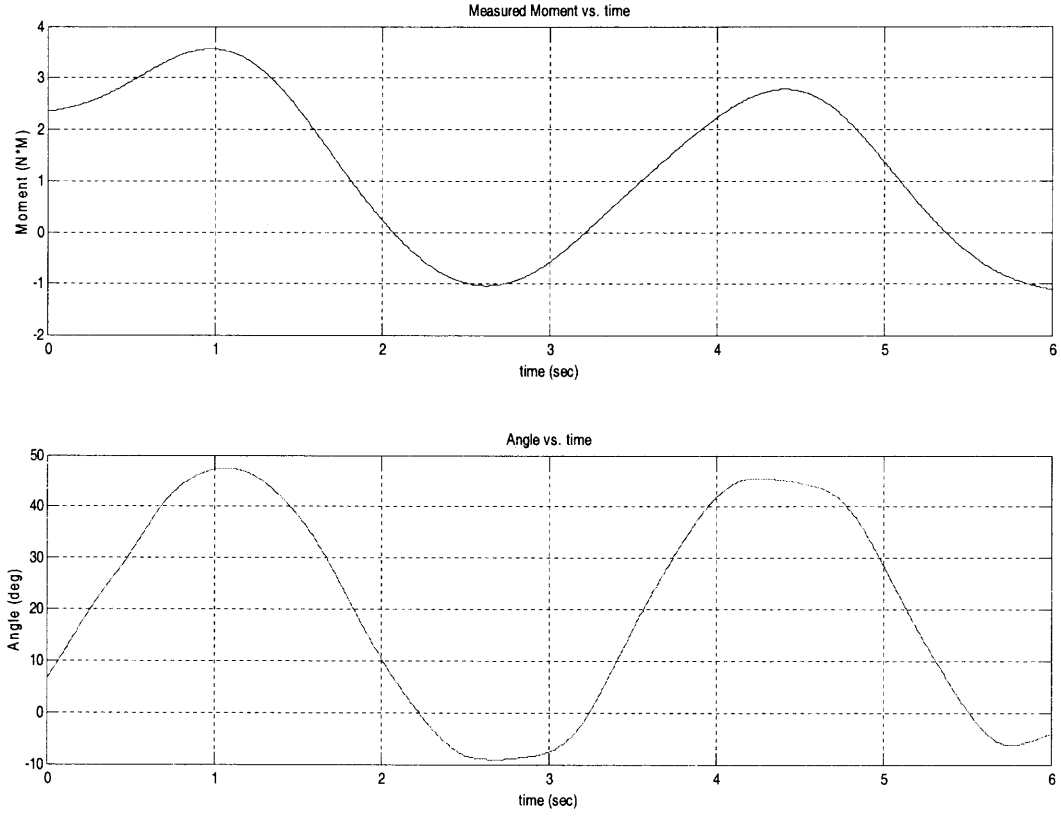

Figure 5.9 Measured moment and angle plots for subject 2 Task 3

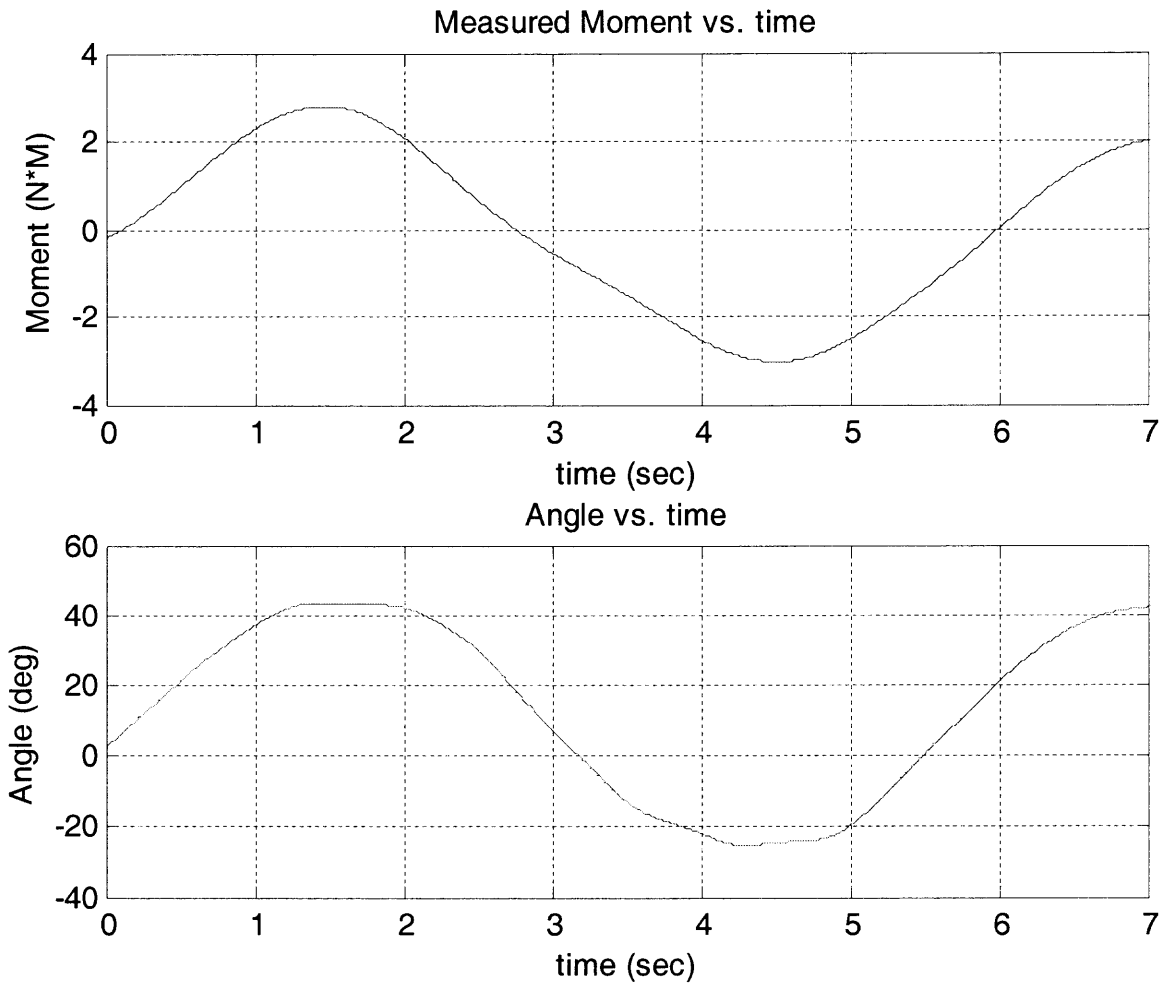

Figure 5.10 Measured moment and angle plots for subject 3 Task 3

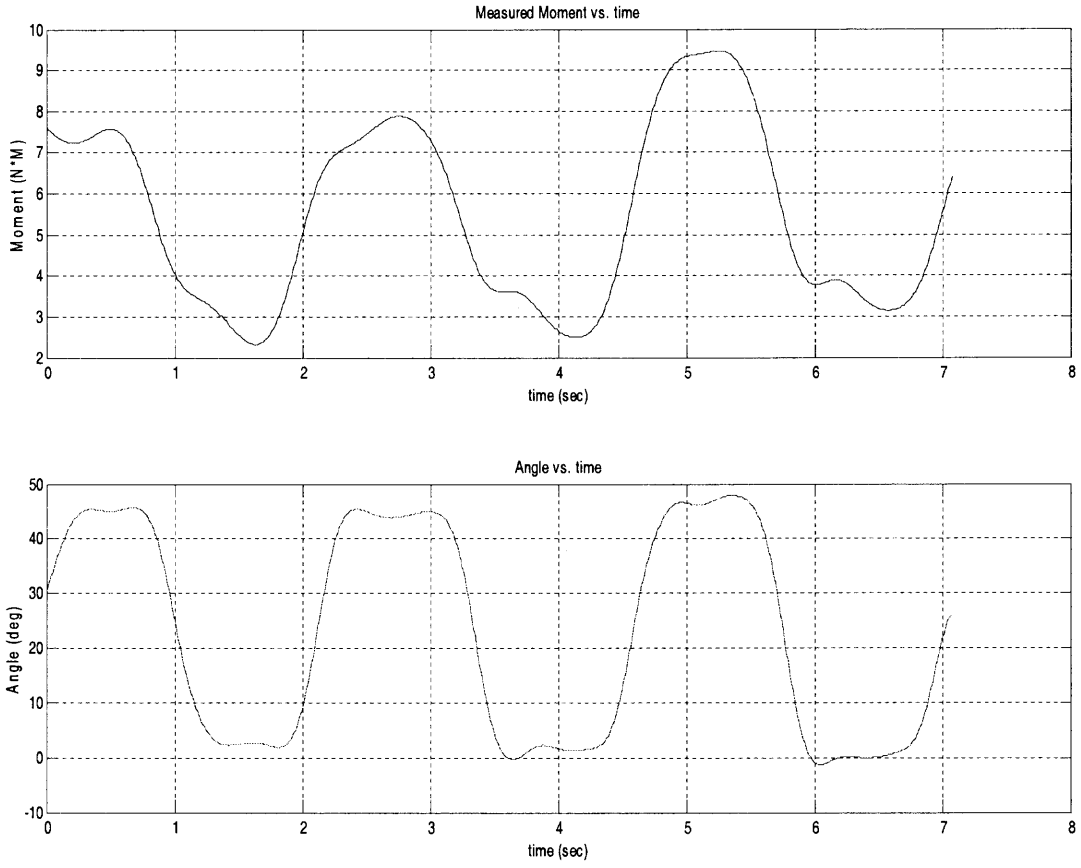

Figure 5.11 Measured moment and angle plots for subject 1 Task 4

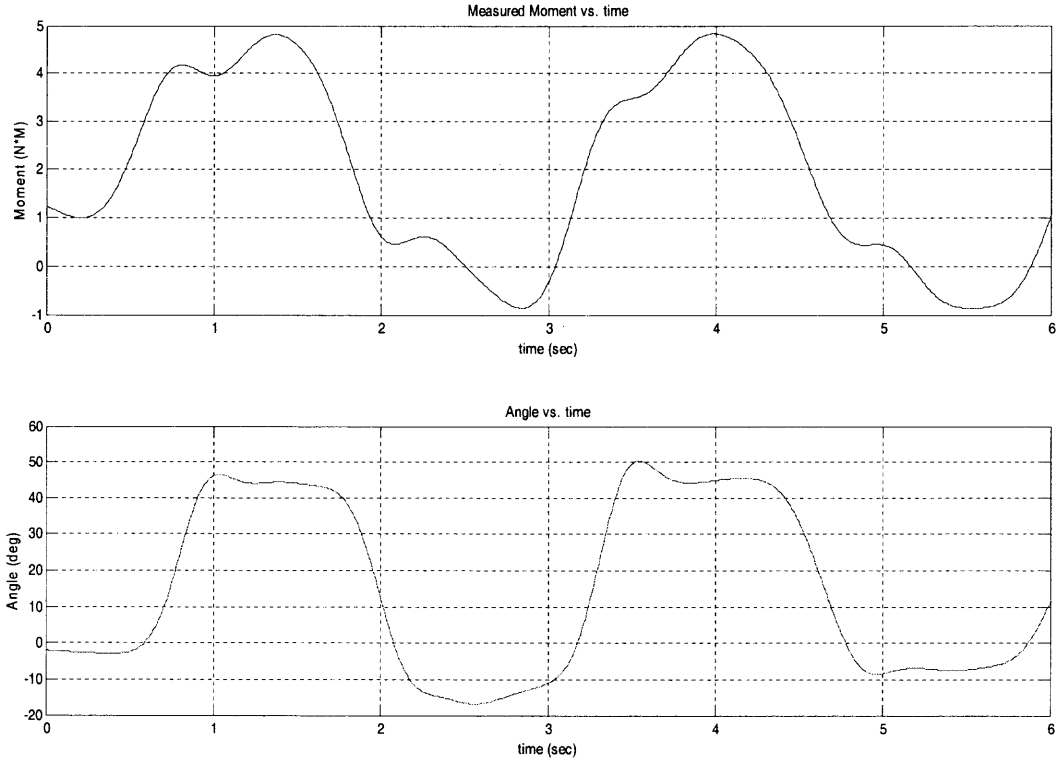

Figure 5.12 Measured moment and angle plots for subject 2 Task 4

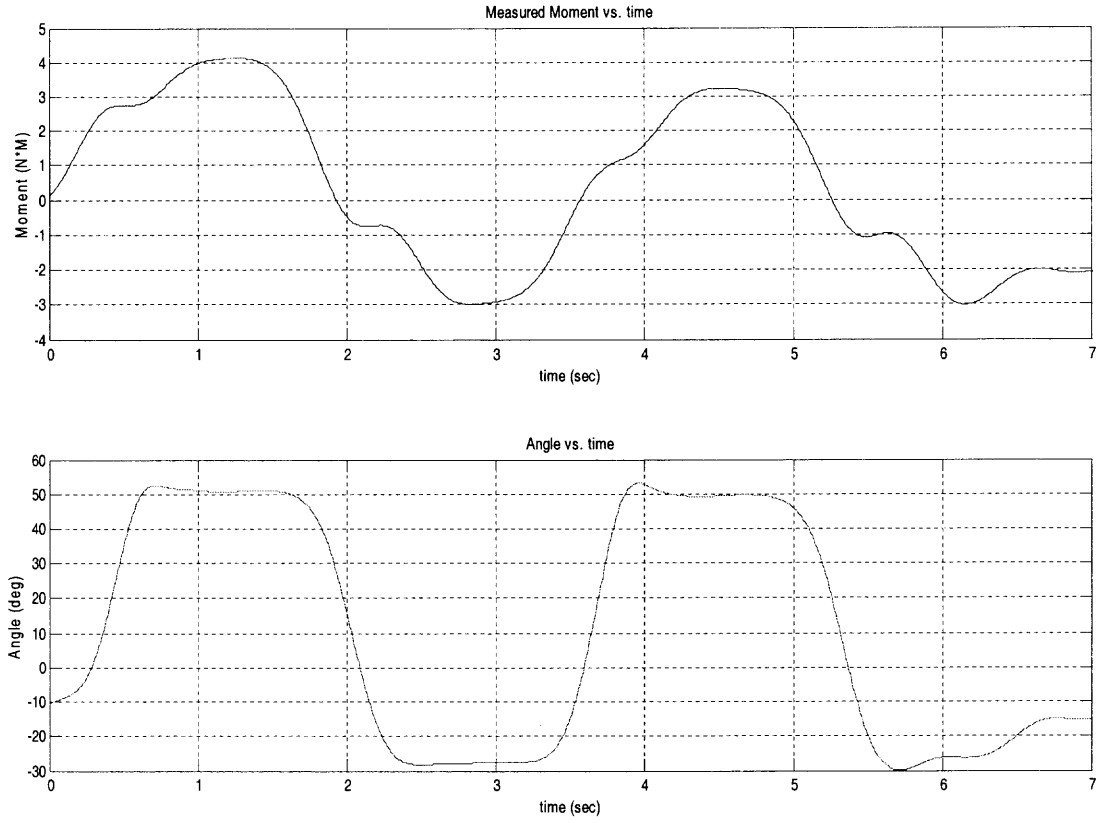

Figure 5.13 Measured moment and angle plots for subject 3 Task 4

CHAPTER 6

DISCUSSION

6.1 Interpretation of results

It can be seen in the calibration plots (Figure 3.2) that as one set of data reaches a maximum, the other set of data reaches a minimum. This is exactly what is expected and needed for this setup to be functional and reliable since it shows that the two pieces of equipment are synchronized. They are mirror images of each other because of the starting location of the angle sensor, as the angle decreases and becomes negative, the normal force on the sensor increases.

For the first task, it is shown that the moments directly correspond to the angle of the limb, and they both increase in unison (Figures 5.2-5.4). This is due to the fact that at the starting angle, where the leg is vertical, there is no gravitational torque that is trying to rotate the lower leg about the knee joint, but as the limb is slowly pulled upward toward horizontal, a steadily increasing force is measured. The gravitational torque plot (red) is directly dependant on the measured angle, so it is to be predicted that the shape of the gravitational torque and the measured angle (blue, bottom graph in Figures 5.2-5.4) are essentially the same, just scaled differently. The measured moment (blue, top graph) in these figures, however, also increases as a function of angle, which is to be predicted for this setup, but is almost exactly equal to the calculated gravitational moment based only on angle measurements. This observation supports a conclusion that under these conditions the inertial, damping, and stiffness torques are close to zero, changing the kinematic equation $M_{applied}=I*\alpha+\beta*\omega+k(\Delta\theta)+m*g*l*\sin(\theta)$ to $M_{applied}= m*g*l*\sin(\theta)$ for

these trials. At the peak of the measured force graph there is a significant overshoot in almost all of the measured force trials. When comparing the measured force vs. angle, it is evident that even though the measured force keeps increasing, the angle does not change. This shows that the end of the range of motion for the lower leg has been reached and the tester continued to pull and is now lifting the mass of both the lower and upper leg segments. For this reason, the measured moment keeps increasing even though the gravitational moment stops increasing at the maximum angle, and a constraint would be a good solution to this issue in future studies.

These plots also show that the lower leg is behaving like a pendulum under slow moving conditions for the first two subjects, and since the calculated gravitational torques are about equal to the measured torque, it can be stated that there is no appreciable torque due to stiffness in the joint. A further demonstration of this observation occurs when the leg of the second subject was slowly pulled to almost horizontal and held for a very long time. The gravitational moment and the measured moment to hold the leg in this manner were nearly equal for all time, as shown in Figure 6.1.

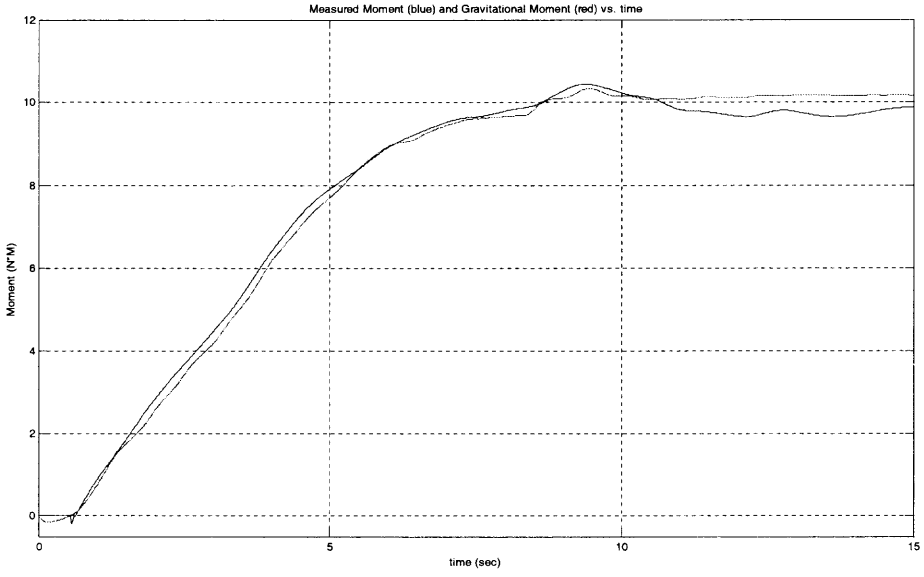

Figure 6.1 Plot of measured moment (blue) and calculated moment (red) vs. time for extended time.

However, the third subject shows some difference between the measured torque and the gravitational torque, and this difference grows as a function of the angle. Since the limb is moving very slowly, this torque cannot be quantified by the inertial torque due to acceleration, or the damping torque due to velocity. This result supports earlier research done by Kate Swift (2006) where she found an extra torque that drove the leg toward vertical with an extra moment during the pendulum knee drop test. The observation that this torque increases as a function of angle and appears to be linear allows it to be modeled as a rotary spring, where the force is governed by a constant stiffness multiplied by the change in angle from the resting point.

Her research also calculated a damping coefficient that when multiplied by the angular velocity in radians per second gives a torque resisting movement due to damping drag. These coefficients ranged in value from .3 to .9, so these two extreme values were

used in this study. Plots of both the maximum (red) and the minimum (blue) damping moments for a Task 2 trial are shown in Figure 6.2

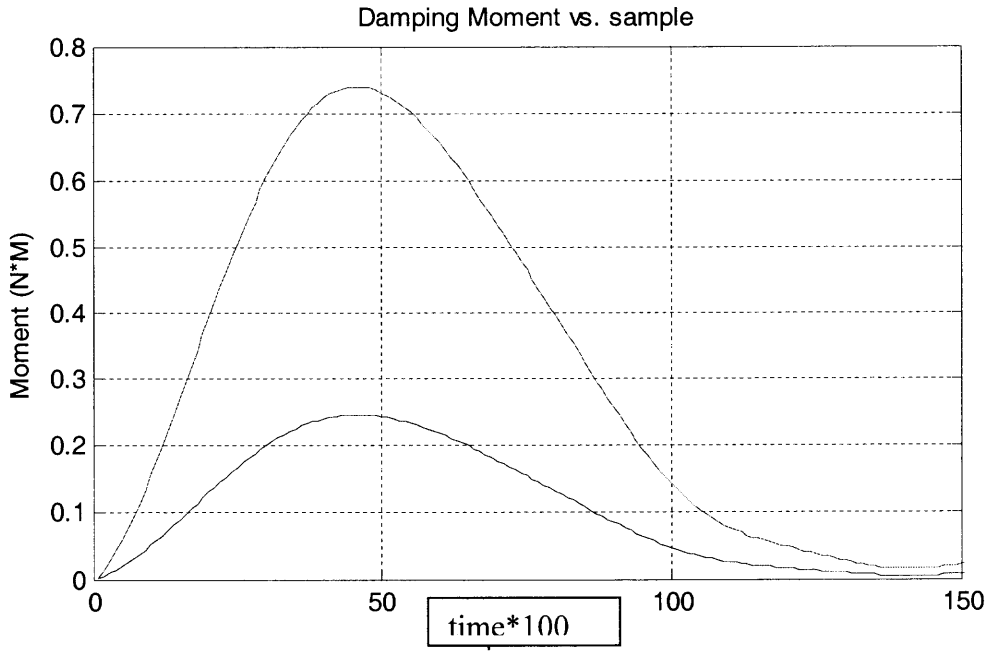

Figure 6.2 Maximum (red) and minimum (blue) damping moments for Task 2 Subject 1

For the second task where the lower leg was pulled with a much higher velocity, similar loading curves were observed. For these trials, it was shown that similar maximum gravitational moments were measured for all subjects when compared to the first task, but a higher measured moment was recorded in all the trials, with the difference from the first to the second trial being 3 N*M for the first subject, 1 N*M for the second subject, and 1.5 N*M for the third subject. When looking at the angular velocity plots, it is evident that the change is angle is occurring at a higher rate than in the first trials (between 65 and 85 deg/s for task 2 compared to between 5 and 16 deg/s for task 1 for all subjects), and that a significant angular acceleration (+84 to –75.5 deg/s^2 for subject 1, +118 to -112 deg/s^2 for subject 2, and +108 to -116 deg/s^2 for subject 3) is occurring

during the loading portions of the curves. Since the kinematic equation has both velocity and acceleration dependant terms that add to the gravitational moment to equal the theoretical measured moment, both of these terms should be taken into account for these trials. As found by Lebiedowska et al (1999). the damping of the knee joint is exceedingly small (B_n=0.06±0.022(Nsrad^{-1} m)) and the measured angular velocity, when converted into radians per second ranges from .85 to 1.26 radians per second, making the force from damping and angular velocity range from .05 to .071 N*M, which is almost insignificant.

The forces caused by angular acceleration and the mass moment of inertia need to be taken into account. For all three trials, the angular acceleration for the lower leg as measured by the angle sensor, differentiated twice, and converted into radians per seconds^2 is between .9 and 1.2 r/s^2 during the fast movement portions of the trials. Also, the mass moments of inertias for the subjects' lower legs are between .88 and 1.31 kg*m^2, so when these terms are multiplied and added to the gravitational moment, it decreases the difference (about 1.0-2.1 N) between the measured and the gravitational moment plots during the loading phase of the curves for all subjects. As with the first trial, it can be seen that the measured force continues to increase well past the time where the end of the range of motion has been reached, indicating that once again the tester continued to pull the leg excessively and began to lift the mass of the upper leg as well.

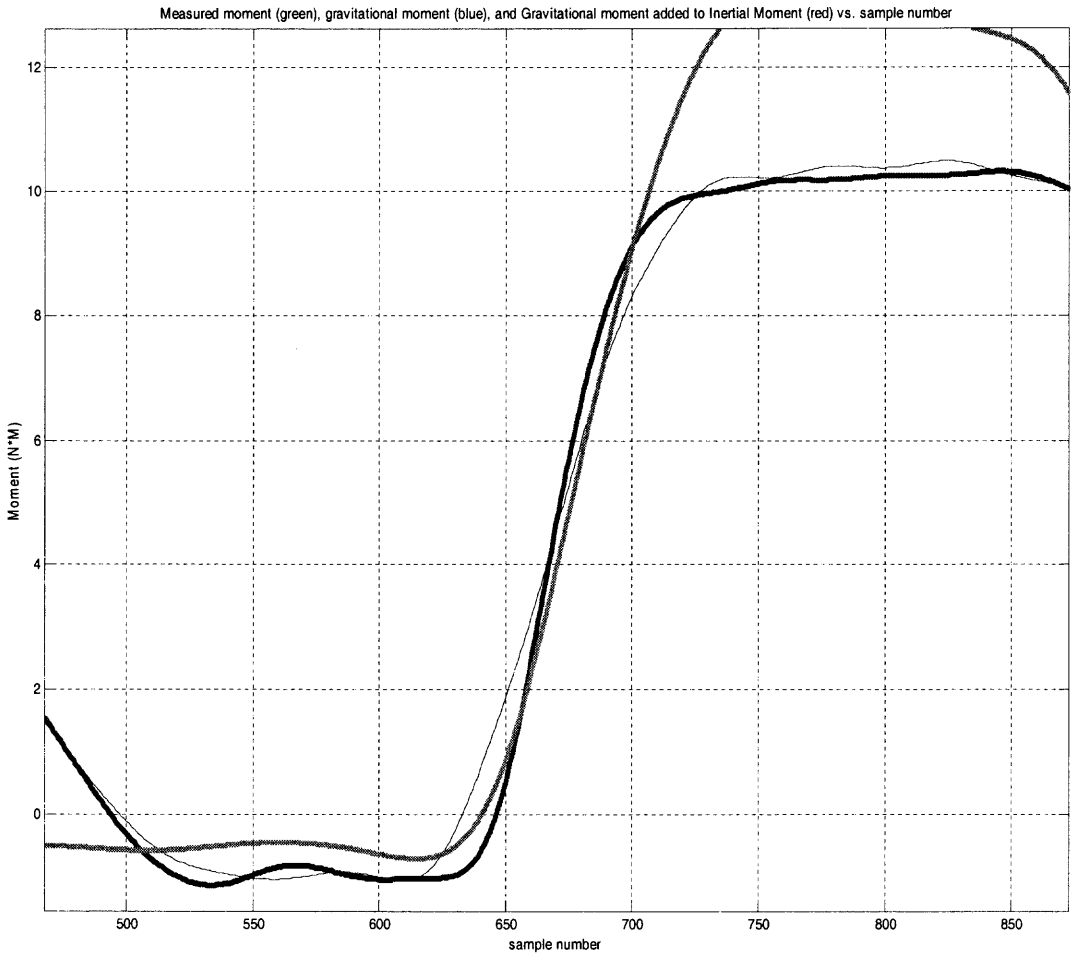

Figure 6.3 Measured moment (green), gravitational moment (blue), and sum of inertial and gravitational moment (red) for subject 1

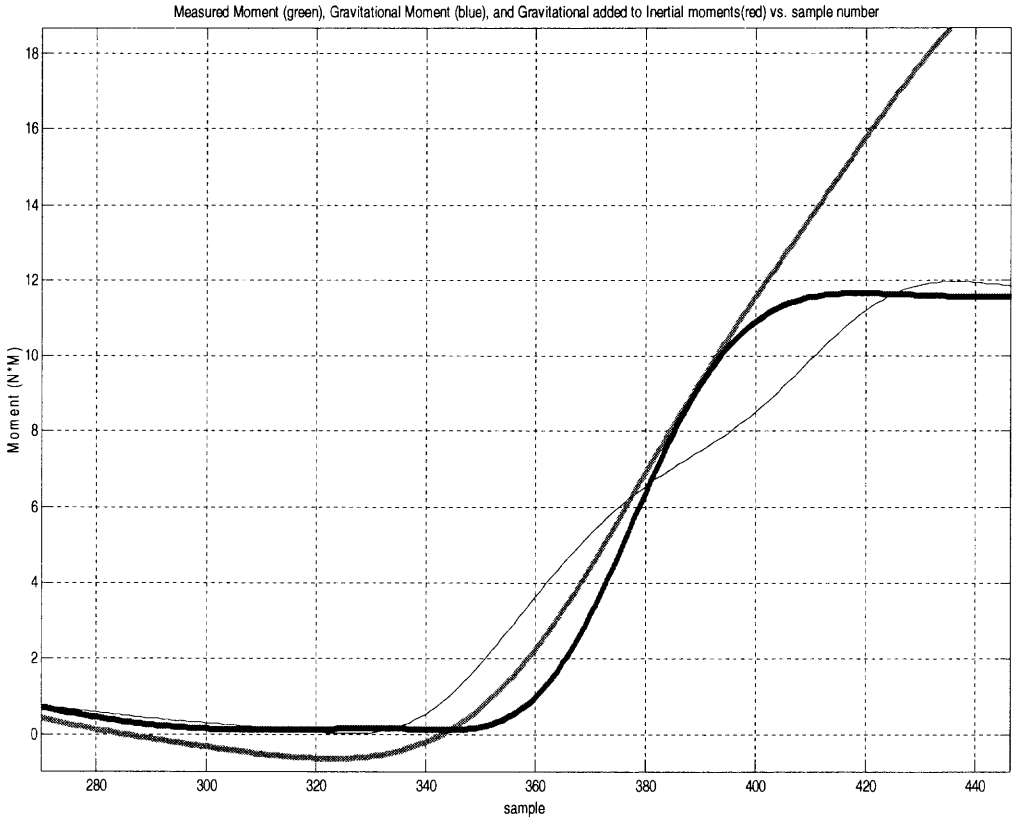

Figure 6.4 Measured moment (green), gravitational moment (blue), and sum of inertial and gravitational moment (red) for subject 3

As apparent from these graphs, the gravitational moment added to the inertial moment (red) more closely resembles the loading portion (slope) of the measured moment (green), but neither match the peak magnitude for the previously explained reason. However, if the damping coefficients of the lower leg that were found by Kate Swift's (2006) research are used, the damping torque can be as high as .75 N*M and as low as .24 N*M. If these torques are included in the kinematic equation and compared to the measured torque, they are slightly closer (.32 N*M) for the majority of the loading segment of the curve in Task 2 as shown in Figure 6.5.

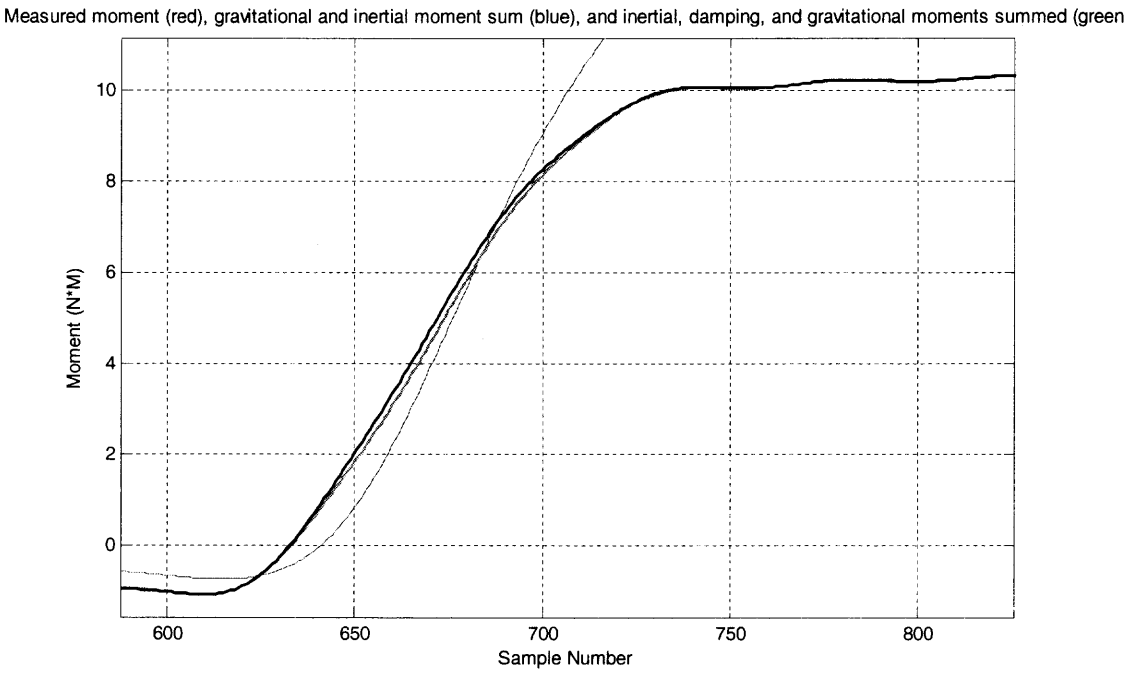

Figure 6.5 Measured moment (red), gravitational moment added to inertial moment (blue), and gravitational, inertial, and damping moments summed (green).

In the case of the third task, it was shown for all trials of all subjects that the measured moment was much lower than any of the tasks where the limb was moved against gravity, on average about four times less force was needed to move the leg in this orientation. It also shows that another degree of freedom used to measure forces (X) while the leg is being supported by the force sensor is capable of measuring the moments to move the leg accurately. Since the subject was aligned horizontally, the force required to move the leg is most likely a combination of overcoming an intrinsic stiffness in the leg and external factors impeding motion such as clothing and friction.

While the fourth task used the same setup as the third task, the moments measured were greater than those in the third since the limb was now being moved at a much greater velocity. The moments were higher since to make the limb move at a higher

speed, a much greater acceleration was needed to reach the desired speeds for this experiment. In the process of accelerating the limb, the force exerted by the tester must overcome the force resisting the movement by the inertial elements of the limb. The inertial force (I*α) will only take on integer values when the limb is accelerating and will equal zero when the limb is at rest as shown by simultaneously plotting measured force (red) on the same axis as the inertial force (blue)

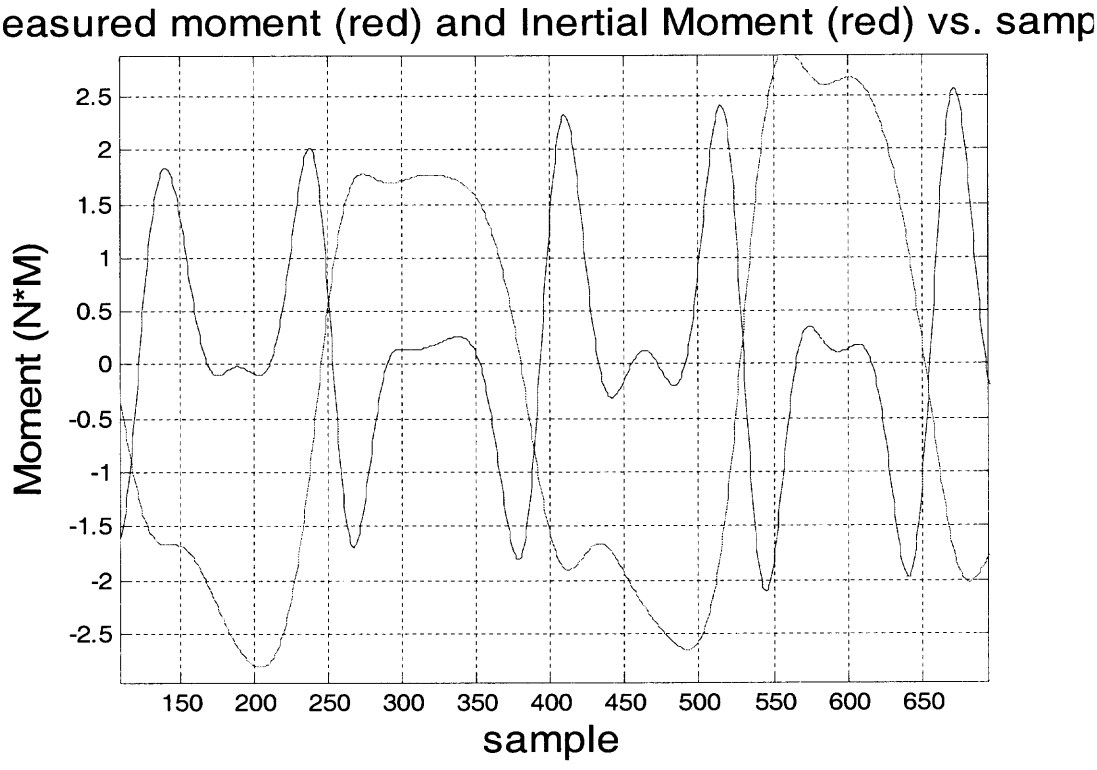

Figure 6.6 Measured moment (red) and inertial moment (blue) for subject 1

Here it is evident that inertial moments are only present as the limb is being pushed in a manner in which it accelerates, and also that the maximum negative force of one variable corresponds to the maximum positive force of another variable and are very close in value when compared in each movement element. The measured moment is

always slightly greater in value than the inertial moment, which can be explained by intrinsic elastic components to the limb or the clothing that the subject was wearing. As this graph and setup for tasks three and four show, the device as it is currently used has enough versatility to be used in various orientations and obtain repeatable measurements that can be predicted by deriving moments from the kinematic equation through the use of angular position data.

Even though research dictates that there is some intrinsic stiffness of the joint caused by a variety of factors, these experiments have had essentially every moment force accounted and solved for while omitting the intrinsic stiffness of the system within some small margin of error. This margin of error can also be explained by the use of an anthropometric table as opposed to actually measuring the distances of the limbs and approximately weighing the limbs for calculations. According to Wang et al. (1993) it has been shown extensively through mechanical testing that muscle, as well as most biological materials exhibit some degree of viscoelasticity. They found that the sarcomere, which is the basic unit of muscle, exhibits the mechanical properties of a dual stage spring over a large range of sarcomere strain lengths. It was concluded that the endo and exosarcomeric lattices behave as viscoelastic force bearing elements. Simply put, when passively strained, a muscle will bear an initial load that will decay over time as the viscoelastic property dictates, but in their study the muscle was displaced a very large amount, much greater than a physiological joint would allow. It is likely that over the operating range of motion of the joint in this study, a high enough strain was not induced on the muscles to have it respond in a way that generates a significant force to resist the movement.

6.2 Further Research and Design Improvements.

The experimental setup and equipment parameters are sufficient to be used as a biomechanical measure that will give a better reliability than a physical therapist subjectively grading patients on a poorly standardized scale. The potential for use on the upper limbs is also very strong. The only changes that need to be made for this to measure the upper limb mechanics are the orientation of the Flock of Birds receiver to keep a consistent zero axis location, and the anthropometric calculations which can be easily changed to find the masses, lengths, centers of mass, and the moments of inertia for the upper limbs.

Predictably, there will be an overall higher amount of torque generated in the limb of a spastic patient under the conditions of passive movement, but a simple measure of joint torque and angle will most likely not suffice in replacing the Modified Ashworth Scale. For the same stretch and velocity, the degree of alpha motor activation may vary between subjects and even within the same subject. Following the concept of recruitment described by Lehman et al. (2004), in voluntary conditions smaller motor units will be activated first, with the larger ones being recruited only as needed. During the stretch reflex activation, it is hard to pinpoint whether larger or smaller motor units are recruited and this can make a very large difference in the magnitude of the torque generated by the muscle during the test. The use of EMG electrodes either implanted or on the surface would give some information on the extent of muscular activation, since it measures the electrical activity of the motor neurons. This setup would be more powerful with EMG information being recorded, but as of now the hardware and software programming limit

the ability to fully integrate three external devices being read serially, all with different sampling rates and port properties, to reconstruct the information vs. time accurately.

Muscle contraction is not only dependant on motor neuron activation, but also calcium ion and ATP levels within the sarcomere. Even if the motor unit is recruited and the muscle depolarizes, the extent and strength of the contraction is dependant on the ability of the actin and myosin to create cross bridges, relative motion, detach, and repeat the process a number of times to shorten the muscle, creating force. Szentesi et al. (2001) explain that the actin and myosin can't bind if the level of calcium is not sufficient in the sarcomere, allowing fewer fibers to create cross bridges and pull, leading to an overall lower muscle force output. Also, if ATP is not present in the cell the cross bridge will not detach, linking the actin and myosin for longer than required. Since the ratchet and pull action has already occurred, another cannot occur unless the cross bridge releases and resets itself, and it needs energy from ATP to achieve this. Not only is muscle force dependant on the recruitment of the muscle fibers by the central nervous system, but is very dependant on the chemistry taking place within the muscle and may be significantly weaker if the subject has poor diet habits or has an overall vitamin deficiency.

Lastly, Ikai et al. (1968) states that muscle force generated is most closely correlated with the overall cross sectional area of the entire muscle belly. Intuitively, this states that a larger muscle will generate a larger force. Since the device created measures the end result of the muscle contracting, there is no way of knowing whether or not a full grown man that generates very high joint torques has more severe spasticity than a young girl that generates much lower torques during her trials. All it can indicate is whether or not the muscle contracted, indicated by a spike in torque. Even if the device is used on

the same person over a long period of time the muscular properties of the subject will likely change over time. For example, if they become increasingly sedentary as their impairment increases their muscles will begin to atrophy, lowering the overall amount of force that they will be able to output. If before each trial the therapist asked the subject to generate a maximum amount of muscle force in extension and flexion the data could be normalized to this. It would probably allow for the quickest and easiest way to create a repeatable, normalized set of conditions if all force readings taken during the trials were presented as a percent of the maximum, but other issues arise from this including muscle fatigue following maximal exertion. Also, it is possible that the potential maximum forces generated could be extremely high and even if the therapist could resist these forces, the instrumentation would likely overload and break. If it is possible to find a force sensor that could withstand very high forces and then accurately measure forces several orders of magnitude smaller without having to be recalibrated then this could be a possible experimental design improvement since it creates a single set of joint torque parameters.

CHAPTER 7

CONCLUSIONS

As shown by the test results, the device developed can be used to obtain a biomechanical assessment of a human limb. The data shows an accurate picture of the nature of the joint torques being applied to the force sensor as the angle changes, as well as the angular velocity and acceleration of the limb. In comparing the measured forces of the torque required to move the limb to the model derived by the kinematic equations, it was evident that the measured force closely resembled what would be predicted by modeling the limb as a pendulum under slow and fast rotation conditions alike. While not precise, the use of the anthropometric tables for calculations in these procedures proved sufficient for calculating masses and lengths of the limbs, as evidenced by the comparison of calculated forces to the measured forces.

When compared to other biomechanical assessments of limbs such as the pendulum knee drop, the assessment in this study differs in the observation that very little torque in the form of damping occurs. Observing the plot of angle vs. time in a pendulum knee drop, it is clear that there is some significant damping force during the dynamic movement as evidenced by the fact that when modeled, a limb damping out due to gravitational torques will oscillate much longer than an actual human trial. Under conditions of this study where the limbs were moved at a high velocity, nearly all of the measured torque was accounted for by the gravitational, damping, and inertial moment, indicating that there is in fact minimal intrinsic stiffness at the joint. While it is evident there is some resistive torque during the horizontal trials, a more precise setup to suspend

the limb horizontally would decrease the torque caused by tester error. Further studies including the use of EMG in these biomechanical assessments could help in determining the level of involuntary muscle activation that may obscure how the joint behaves, as well as the extent of the intrinsic stiffness of the joint when a more accurate horizontal setup is developed.

APPENDIX A

MATLAB SOURCE CODE FOR DATA COLLECTION

```
clear all
SubjectCode=1;
warning off all

%%%%%%%%%%%%%%
%FOB
%%%%%%%%%%%%%%
C = serial('COM5');
set(C,'BaudRate',115200);
set(C,'InputBufferSize',100000);
set(C,'OutputBufferSize',100000);
fopen(C);
pause(1)

fobtime=[];
FOBread=[];
FT=[];
Ftread=[];

% CHECK STATUS
% Aquire a known value to confirm that Flock is open
P=[79 2];   %Examine value of bird status, 2 bytes should be returned
fwrite(C,P);
pause(.5);
fportstatus=C.BytesAvailable;

if fportstatus == 0;
    disp('Error: Bird is not flying')
    fclose(C)
    delete(C)
    return  %Abort program if error
end

% SET MEASUREMENT/SAMPLE RATE TO 100 S/SEC.
% 80 is change value command, 7 is the measurement rate
% 0 is the lsb of new rate measurement, 100 is the msb new rate
measurement
% 0  100 sets measurement rate to 100 f/s.
Q=[80 7 0 100];
fwrite(C,Q);

%FILTER OFF
T=[80 4 7 0]; %80 is change value, 4 is filter, 7 if off all, 0 is msb
fwrite(C,T);

% VERIFY MEASUREMENT/SAMPLE RATE
% 79 examines value, 7 is new measurement rate
```

```
L=[79 7];
fwrite(C,L);
pause(.1);
d=C.BytesAvailable;
NewMeasurementRate = fread(C,d);

%%%%%%%%%%%%%%
%FT
%%%%%%%%%%%%%%
A = serial('COM1','BaudRate',38400,'DataBits',8);
set(A,'Parity','none');
set(A,'FlowControl','software');
set(A,'Stopbits',1);
set(A,'Terminator',13);
set(A,'InputBufferSize',100000);
set(A,'OutputBufferSize',100000);
fopen(A);
%fprintf(A,'CD R'); %Resolved force output

% fprintf(A,'SU');%Sensor unbias
% fprintf(A,'SB');%Sensor bias

fprintf(A,'CF 1') %Communication fast
fprintf(A,'CV 7') % Enabling only Fxyz output
fprintf(A,'CL 1')
%fprintf(A,'FC 1') %Enabling filter clock
 % FOB Purge buffer just before data collection starts
fprintf(A,'SF 100') % frame rt
q=A.BytesAvailable;  %Remove junk above
if q>0
    junkf=char(fread(A,q));
end

% FT Purge buffer just before data collection starts
r=C.BytesAvailable;  % Check FOB buffer for junk
if r>0
    junkf=fread(C,r);
end

pause(1);

%%%%%%%%%%%%%%%%%%%%%%%%%
% START DATA COLLECTION
%%%%%%%%%%%%%%%%%%%%%%%%%
beep
fwrite(C, 87); % FOB 87 is angle only 89 is position and angles
fwrite(C,64); % Start FOB streaming
fprintf(A,'QS'); %Stream start FT

pause(1)

% FOB Purge buffer just before data collection starts
% FT Purge buffer just before data collection starts
r=C.BytesAvailable;
q=A.BytesAvailable; % Check FOB buffer for junk
```

```
if r>0 & q>0
    junkf=fread(C,r);
    junka=fread(A,q);
end

% FOB/FT data ® loop
 display('Start Data Collection');
tic
pause(15)  %Run for 15 seconds
z=toc;
fwrite(C,66); % FOB stream stop
fprintf(A,'QR'); %FT stream stop

display('Collection Stopped');

beep
Ftread=fread(A);  %Read FT
FOBread = fread(C); %Read FOB

%%%%%%%%%%%%%%%%%%%
%CLOSE PORTS
%%%%%%%%%%%%%%%%%%%

% FOB
fclose(C);   %FOB
delete(C);
clear C
fclose(A);   %FT
delete(A);
clear A

%%%%%%%%%%%%%%%%%%%
%UNPACK
%%%%%%%%%%%%%%%%%%%

%FOB unpack
FOB=FOBread;
i=1;
j=1;
size=length(FOB);
while i<size
    if FOB(i)>128 % Checks to see if there is a synchronization bit
        FOBL(i)=FOB(i)-128; % Stripping off □ime□ronization bit
    else
        FOBL(i)=FOB(i);% Does nothing
    end
   FOBL(i)=bitshift(FOBL(i),1); % Shifts LS byte one bit left
   F(j)=256*FOB(i+1)+FOBL(i); % Combines LS and MS bytes into 16 bit
word
   F(j)=bitshift(F(j),1); % Shifts whole word left one bit left
   j=j+1;
   i=i+2; % Increments by 2
end

for j=1:length(F)
```

```
    if F(j)> 32767
        F(j)=(F(j)-65535);
    else
        F(j)=F(j);
    end
end
    Xa=zeros;
    Ya=zeros;
    Za=zeros;
    k=1;
    F=F';

%Creating X, Y, Z column vectors

for i=1:((length(F))/3)
  X(k)=F(i*3-2);
  X=X';
  Xa=((X*180)/32768); % bird conversion Aactor Aor millimeters;
  Xa=Xa';
  Y(k)=F(i*3-1);
  Y=Y';
  Ya=((Y*180)/32768);
  Ya=Ya';
  Z(k)=F(i*3);
  Z=Z';
  Za=((Z*180)/32768);
  Za=Za';
  k=k+1;
end

%FT unpack
f=Ftread;
FOBrt=length(Ya)/z;
FORCErt=length(char(f'))/24/z;
f1=Ftread;
f1=char(f1);
f1=f1';

b=find(f==6);
a=find(f==10);
f(((b(1))):length(f))=[];
f(1:a(1))=[];
ff=char(f);
ff=ff';
fn=str2num(ff);

endvalue=((a(1)/24)*(FOBrt/FORCErt));
endvalue=round(endvalue);

Xa1=Xa;Ya1=Ya;Za1=Za;
Xa1(1:endvalue)=[];
Ya1(1:endvalue)=[];
Za1(1:endvalue)=[];
Fx=fn(:,2);
Fy=fn(:,3);
Fz=fn(:,4);
```

```
ftl=length(Fz);
foblen=length(Ya1);
fobsam=foblen/z;
fobfr=1/fobsam;
fts=ftl/z;
ftfr=1/fts;
timefob=0:fobfr:z;
timeft=0:ftfr:z;
timefob1=0:.01:z;
timeft1=0:.02:z;
[aa bb]=butter(2,.1);%filter 2nd order lpf 10Hz cutoff
[cb db]=butter(2,.05);%filter 2nd order lpf 10Hz cutoff
[cc dd]=butter(2,.07);
[ee ff]=butter(2,.06);
Fzf=filtfilt(aa,bb,Fz);
Fyf=filtfilt(aa,bb,Fy);
Fxf=filtfilt(aa,bb,Fx);
Yaf=filtfilt(cb,db,Ya1);
Xaf=filtfilt(cb,db,Xa1);
Zaf=filtfilt(cb,db,Za1);

r=1;
for i=1:(length(Fzf))
    Forcevec(i)=sqrt(Fzf®^2+Fyf®^2+Fxf®^2);
    r=r+1;
end
Forcevecf=filtfilt(cb,db,Forcevec);
time=(length(Ya)/FOBrt);
timee2=(100./FOBrt)*(length(Ya)/FOBrt);
tmee=length(Fz)/FORCErt;
tmeee=0:(1/FORCErt):tmee;
timeee=0:(1/FOBrt):□ime;
y=1;
%%% Computing and filtering the angular velocities with respect to axes
for i=2:(length(Xa1)-1); %derivative function
     Xvel(y)=(Xa1(i)-Xa1(i-1))./((timeee(i+1)-timeee(i-1)));
     y=y+1;
 end
 Xvell=filtfilt(ee,ff,Xvel);

 y=1;
 for i=2☹length(Yaf)-1); %derivative function
     Yvel(y)=(Yaf(i)-Yaf(i-1))./((timeee(i+1)-timeee(i-1)));
     y=y+1;
 end
 Yvell=filtfilt(ee,ff,Yvel);

 y=1;
 for i=2☹length(Za1)-1); %derivative function
     Zvel(y)=(Za1(i)-Za1(i-1))./((timeee(i+1)-timeee(i-1)));
     y=y+1;
 end
 Zvell=filtfilt(ee,ff,Zvel);
```

APPENDIX B

MATLAB SOURCE CODE FOR DATA PROCESSING

```
%load all forces, angles, and ang vel for sample before running and
%workspaces
weight=??; %enter subject's weight in pounds
height=??; %enter subject's height in inches
mass=weight/2.2;
heightcm=height*2.54;
Llegfootw=.061*mass;
Llegl=(.285-.039)*heightcm*.01;
Llegfootl=(.285)*heightcm*.01;
COMl=.606*Llegfootl;
I=Llegfootw*(.735*Llegfootl)^2+Llegfootw*(.606*(Llegfootl))^2;
Ya11a=Ya11-Ya11(1); %Sets starting leg position as zero point
Ya2a=Ya2-Ya2(1);
Ya3a=Ya3-Ya3(1);
Ya4a=Ya4-Ya4(1);
[aa bb]=butter(2,.25);%filter 2nd order lpf 10Hz cutoff
[cb db]=butter(2,.05);%filter 2nd order lpf 10Hz cutoff
[cc dd]=butter(2,.07);
[ee ff]=butter(2,.06);
[gg hh]=butter(2,.02);

timee=length(Yv3)/FOBrt;% use longest Yv#
tmee=length(F1)/FORCErt;
tmeee=0:(1/FORCErt):tmee;
timeee=0:(1/FOBrt):timee;

Yvv1=Yv1;%/180*pi;
Yvv2=Yv2;%/180*pi;
Yvv3=Yv3;%/180*pi;
Yvv4=Yv4;%/180*pi;

F1N=(F1/100)*9.8;  %converts from counts to newtowns
M1=(F1N*Llegl); %creates a moment vector

%Compute all angular accelerations
y=1;
for i=2:(length(Yvv1)-1); %derivative function
     Yaccel1(y)=(Yvv1(i)-Yvv1(i-1))./((timeee(i+1)-timeee(i-1)));
     y=y+1;
end
Yaccelf1=filtfilt(ee,ff,Yaccel1);

F2N=(F2/100)*9.8;
M2=(F2N*Llegl);

y=1;
for i=2:(length(Yvv2)-1); %derivative function
     Yaccel2(y)=(Yvv2(i)-Yvv2(i-1))./((timeee(i+1)-timeee(i-1)));
```

```
     y=y+1;
end
Yaccelf2=filtfilt(ee,ff,Yaccel2);

F3N=(F3/100)*9.8;
M3=(F3N*Llegl);

y=1;
for i=2:(length(Yvv3)-1); %derivative function
     Yaccel3(y)=(Yvv3(i)-Yvv3(i-1))./((timeee(i+1)-timeee(i-1)));
     y=y+1;
end
Yaccelf3=filtfilt(ee,ff,Yaccel3);

F4N=(F4/100)*9.8;
M4=(F4N*Llegl);

y=1;
for i=2:(length(Yvv4)-1); %derivative function
     Yaccel4(y)=(Yvv4(i)-Yvv4(i-1))./((timeee(i+1)-timeee(i-1)));
     y=y+1;
end
Yaccelf4=filtfilt(ee,ff,Yaccel4);

M1f=filtfilt(gg,hh,M1);
M2f=filtfilt(gg,hh,M2);
M3f=filtfilt(gg,hh,M3);
M4f=filtfilt(gg,hh,M4);

%angles into radians
Yr1=Ya11a/180*pi;
Yr2=Ya2a/180*pi;
Yr3=Ya3a/180*pi;
Yr4=Ya4a/180*pi;

%gravitational moment mglsin(theta)
Mnet1=Llegfootw*9.8*COMl*sin(Yr1);
Mnet2=Llegfootw*9.8*COMl*sin(Yr2);
Mnet3=Llegfootw*9.8*COMl*sin(Yr3);
Mnet4=Llegfootw*9.8*COMl*sin(Yr4);

%Inertial Moment
Ia1=I*Yaccelf1/180*pi;
Ia2=I*Yaccelf1/180*pi;
Ia3=I*Yaccelf3/180*pi;
Ia4=I*Yaccelf4/180*pi;

%Sum of inertial and gravitational moments
II1=Ia1+Mnet1(1:length(Ia1));
II2=Ia2(1:length(Mnet2))+Mnet2;
II3=Ia3+Mnet3(1:length(Ia3));
II4=Ia4+Mnet4(1:length(Ia4
```

REFERENCES

1. Allison, S., & Abraham, L. (1995) "Correlation of quantitative measures with the modified Ashworth scale in the assessment of plantar flexor spasticity in patients with traumatic brain injury." Journal of Neurology. 242:699-706.

2. Ashworth, B. (1964). "Preliminary trial of carisoprodol in multiple sclerosis." Practitioner. 192:540-2.

3. Bax, M., Goldstein, M., & Rosenbaum, P. (2005). "Proposed definition and classification of cerebral palsy," Developmental medicine and child neurology 47 (8): 571-576.

4. Blackburn, M., van Vliet, P., & Mockett, S. (2002) "Reliability of measurements obtained with the Modified Ashworth Scale in the lower extremities of people with stroke." Physical Therapy., 82: (1) 25-34.

5. Bohannon, R.W., & Smith, M.B. (1987). "Interrater reliability of a modified Ashworth scale of muscle spasticity. Physical Therapy., 67: 206-207.

6. Botterman, B. R., Binder, M. D., & Stuart, D. G. (1978). "Functional anatomy of the association between motor units and muscle receptors" American Zoologist 18(1):135-152.

7. Boyd, R.N., Ada, L. Barnes, M., & Johnson, G. (2002). "Upper motor neurone syndrome and spasticity" Clinical management and neurophysiology Cambridge University Press; 2002. p. 96-121.

8. Boyd, R.N., & Graham, H.K. (1999). "Objective measurement of clinical findings in the use of botulinum toxin type A for the management of children with cerebral palsy." European Journal of Neurology. Suppl 4:S23-35.

9. Brashear, A. (2002) "Inter- and intrarater reliability of the Ashworth Scale and the Disability Assessment Scale in patients with upper-limb poststroke spasticity." Arch Phys Med Rehabil. 83:1349-54.

10. Damiano, D., Guinlivan, J., Owen, B., Payne, P., Nelson, K., & Abel, M. (2002). "What does the Ashworth scale really measure and are instrumented measures more valid and precise?" Developmental Medicine & Child Neurology, 44: 112-118.

11. Filippi, G., Errico, P., Santarelli, R., Bagonlini, B., & Manni, E. (1993). "Botulinum A toxin effects on rat jaw muscle spindles." Acta oto-laryngologica. 113(3):400-404.

12. Hevers, W., & Lüddens, H. (1998). "The diversity of $GABA_A$ receptors. pharmacological and electrophysiological properties of $GABA_A$ channel subtypes" Mol. Neurobiol. 18 (1): 35-86.

13. Ikai, M., & Fukunaga, T. (1968). "Calculation of muscle strength per unit cross-sectional area of human muscle by means of ultrasonic measurement" European Journal of Applied Physiology (26); 1.

14. Jobin, A., & Levin, M. (2000). "Regulation of stretch reflex threshold in elbow flexors in children with cerebral palsy: a new measure of spasticity." Developmental Medicine & Child Neurology, 42: 531-540.

15. Lebiedowska, M. K., & Fisk, J. R. (1999). "Passive dynamics of the knee joint in healthy children and children affected by spastic paresis" Clinical Biomechanics 14(9): 653-660.

16. Lehman, G. J., Lennon, D., Tresidder, B., Rayfield, B.,& Poschar, M. (2004). "Muscle recruitment patterns during the prone leg extension" BMC Musculoskelet Disord. 2004; 5:3.

17. Leo, R. J., & Baer, D.(1992) "Delirium associated with Baclofen withdrawal: A review of common presentations and management strategies." Psychosomatics: The Journal of Consultation and Liaison Psychiatry. 46(6), 503-507.

18. McLean, M.J., Macdonald, R.L., (1988). "Benzodiazepines, but not beta carbolines, limit high frequency repetitive firing of action potentials of spinal cord neurons in cell culture." J Pharmacol Exp Ther. 244 (2): 789-95.

19. National Institute of Neurological Disorders and Stroke (2002). Cerebral Palsy Information Page [Information posted on Website National Institutes for Health] Retrieved November 28, 2007 from the World Wide Web: http://www.ninds.nih.gov/disorders/cerebral_palsy/cerebral_palsy.htm.

20. Pandyan, A. D., Price, C.I.M., Rodgers, H., Barnes, M.P., & Johnson, G.R. (2001). "Biomechanical Examination of a commonly used measure of spasticity." Clinical Biomechanics., 16: (10) 859-65.

21. Patrick, E., & Ada, L. (2006). "The Tardieu Scale differentiates contracture from spasticity whereas the Ashworth Scale is confounded by it." Clinical *Rehabilitation* (2) : 173-182.

22. Pisano, F., Miscio, G., Del Conte, C., Pianca, D., Candeloro, E., & Colombo, R. (2000). "Quantitative measures of spasticity in post-stroke patients," Clnical Neurophysiology. 11:1015-1022.

23. Swift, K., (2006) "Inverse dynamic modeling for the characterization of spasticity." Presented to the staff of NJIT, January 2006.

24. Szentesi, P., Zaremba, R., van Mechelen, W., & Stienen, G. J. M. (2001). "ATP utilization for calcium uptake and force production in different types of human skeletal muscle fibres" Journal of Physiology (531)2: 393-403.

25. Tardieu, G., Shentoub, S., & Delarue, R. (1954). "A la recherché d'une technique de measure de la spasticite." Revue Neurologie ;91:143-4.

26. Wang, K., McCarter, R., Wright, J., Beverly, J., & Ramirez-Mitchell, R. (1993). "Viscoelasticity of the sarcomere matrix of skeletal muscles. The titin-myosin composite filament is a dual-stage molecular spring." Biophysical Journal, April; 64(4): 1161–1177.

27. Widmaier, E., Raff, H., & Strang, K. (2004). Human Physiology (9th ed.). New York: Mcgraw-Hill Higher Ed. 34-62, 207-301.

28. Winter, D. (2005). Biomechanics and Motor Control of Human Movement (3rd ed.). Hoboken, New Jersey: John Wiley and Sons, Inc., 59-102.